JACS
JOURNAL OF THE AMERICAN CHEMICAL SOCIETY
pubs.acs.org/JACS
Perspective

# Radical Sorting Catalysis via Bimolecular Homolytic Substitution ($S_H2$): Opportunities for C($sp^3$)−C($sp^3$) Cross-Coupling Reactions

Iona M. McWhinnie,[†] Robert T. Martin,[†] Jiaxin Xie,[†] Ruizhe Chen, Cesar N. Prieto Kullmer, and David W. C. MacMillan*

Cite This: J. Am. Chem. Soc. 2025, 147, 23351−23366
Read Online
ACCESS | Metrics & More | Article Recommendations

**ABSTRACT:** The development of efficient C($sp^3$)−C($sp^3$) cross-coupling methods that expand access to a pharmaceutically relevant three-dimensional chemical space represents a key frontier in organic synthesis. Traditional cross-coupling strategies readily achieve C($sp^2$)−C($sp^2$) and C($sp^2$)−C($sp^3$) bond formation but face significant challenges in C($sp^3$)−C($sp^3$) coupling due to issues of sluggish inner sphere reductive elimination, $\beta$-hydride elimination, and limited cross-selectivity. Recent advances in C($sp^3$)−C($sp^3$) cross-coupling have highlighted the potential of an alternative bond-forming mechanism, bimolecular homolytic substitution ($S_H2$), as an outer sphere pathway to overcome these limitations. This strategy leverages a "radical sorting effect", in which sterically distinct alkyl radicals are partitioned based on their substitution patterns. This perspective provides a comprehensive analysis of $S_H2$-mediated C($sp^3$)−C($sp^3$) cross-coupling reactions from 2021 to 2024, focusing on iron, nickel, and cobalt catalysis and their powerful applications in quaternary carbon center (QCC) formation. We also highlight emerging opportunities in single functional group cross-coupling and alkene functionalization, demonstrating the versatility of $S_H2$ in accessing complex molecular architectures from abundant feedstock chemicals. By addressing key challenges in C($sp^3$)−C($sp^3$) cross-coupling, $S_H2$ radical sorting catalysis holds significant promise for expanding the C($sp^3$)-rich chemical space and enabling transformative advances in organic synthesis.



## 1. INTRODUCTION

The introduction of novel methods for the efficient construction of carbon−carbon bonds remains a fundamental goal of organic synthesis. Traditional cross-coupling reactions forge carbon−carbon bonds between organic electrophiles and nucleophilic organometallic reagents,[1] enabling the construction of challenging C($sp^2$)−C($sp^2$) and C($sp^2$)−C($sp^3$) bonds through the classic sequence of oxidative addition, transmetalation, and reductive elimination (Figure 1a).[2] In recognition of the revolutionary impact of these powerful transformations, Heck, Negishi, and Suzuki were awarded the 2010 Nobel Prize in Chemistry "for palladium-catalyzed cross-couplings in organic synthesis."[3] Today, there is growing interest in extending the scope of this mechanistic framework to the coupling of two $sp^3$-hybridized substrates.[4,5] Organic molecules with C($sp^3$)−C($sp^3$) bonds exhibit enhanced three dimensionality over their C($sp^2$)-rich counterparts, a structural feature that is well understood to impart desirable pharmaceutical properties and correlate with higher rates of clinical success.[6,7] The introduction of efficient methods for C($sp^3$)−C($sp^3$) cross-coupling can facilitate expanded access to the C($sp^3$)-rich chemical space and holds immense value for drug discovery.

While some traditional electrophiles (e.g., alkyl halides) and nucleophilic organometallic reagents have been employed in C($sp^3$)−C($sp^3$) cross-coupling reactions,[8] multiple challenges, including facile $\beta$-hydride elimination and the limited availability of coupling partners, have hindered the widespread adoption of palladium-catalyzed C($sp^3$)−C($sp^3$) cross-cou-

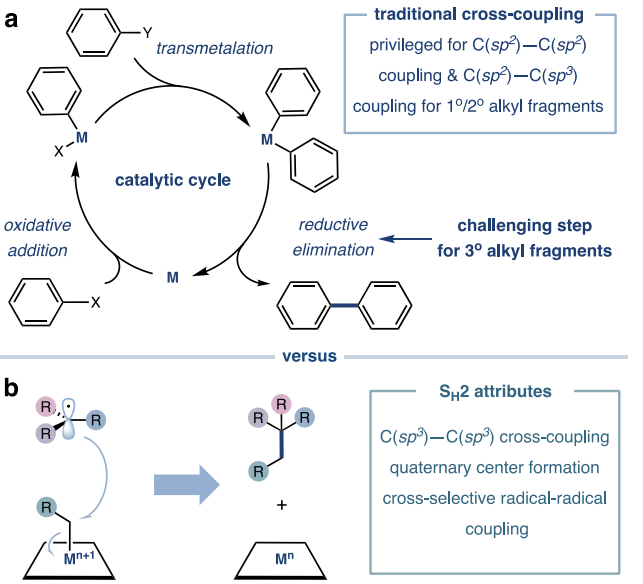


**Figure 1.** (a) Traditional cross-coupling versus (b) radical cross-coupling via bimolecular homolytic substitution ($S_H2$).

**Received:** May 1, 2025
**Revised:** June 20, 2025
**Accepted:** June 23, 2025
**Published:** June 29, 2025





https://doi.org/10.1021/jacs.5c07367
J. Am. Chem. Soc. 2025, 147, 23351−23366

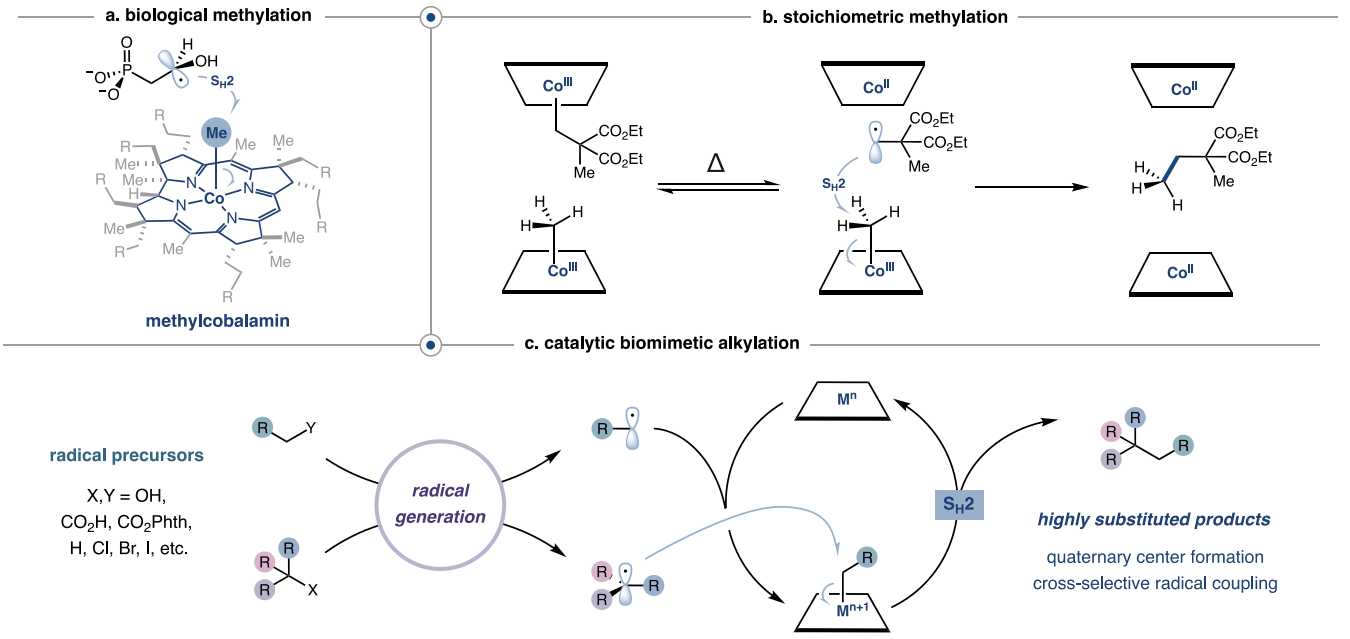


**Figure 2.** (a) C($sp^3$)−H methylation with methylcobalamin via $S_H2$. (b) Stoichiometric $S_H2$ reactions with organocobalt porphyrins via $S_H2$. (c) Design of a biomimetic C($sp^3$)−C($sp^3$) bond formation via transition-metal-mediated $S_H2$ catalysis.

plings.[9] Consequently, considerable effort has been directed toward developing new catalysts and ligands and utilizing abundant alkyl coupling partners with a greater structural diversity.[5,10] First-row transition metals, such as nickel,[5] copper,[11] iron,[12] and cobalt,[13] have gained prominence due to their slower rates of $\beta$-hydride elimination. Notably, these metals are also able to engage in single-electron processes and thus promote radical reactivity. With the rise of photoredox and electrocatalysis, a broader range of native functionalities, including carboxylic acids, alcohols, and C−H bonds, can now be readily activated to serve as $sp^3$-derived radical cross-coupling partners, thereby enabling more versatile C($sp^3$)−C($sp^3$) cross-coupling reactions.[14,15] Despite these advances, radical C($sp^3$)−C($sp^3$) cross-couplings remain underdeveloped compared to reactions involving C($sp^2$) partners. This is largely due to limitations in the traditional mechanistic framework, especially oxidative addition and reductive elimination. For example, while radicals undergo facile single-electron oxidative addition to first-row transition metals, more highly substituted alkyl radicals generally display a diminished binding affinity, as steric hindrance serves to weaken the metal−carbon bond.[16] This issue, combined with slow inner-sphere reductive elimination[17] and side reactions such as $\beta$-hydride elimination, homocoupling, and radical disproportionation,[18] presents substantial challenges in achieving selective and productive C($sp^3$)−C($sp^3$) bond formation. Furthermore, the construction of quaternary carbon centers (QCCs) via C($sp^3$)−C($sp^3$) cross-coupling remains a significant challenge, as bulky 3° alkyl coupling partners are more susceptible to $\beta$-hydride elimination.[19] The ability to efficiently construct complex QCCs through cross-coupling reactions with readily available precursors would represent a transformative advancement in synthetic chemistry.

Given the inherent challenges associated with the inner sphere reductive elimination pathway in traditional C($sp^3$)−C($sp^3$) cross-coupling reactions, alternative mechanisms may provide new avenues for achieving high cross-selectivity and efficient QCC formation. One particularly promising mechanism is bimolecular homolytic substitution ($S_H2$), the radical analogue of the $S_N2$ mechanism (Figure 1b). In nature, the methyltransferase cofactor methylcobalamin carries out biological C($sp^3$)−H methylation through a distinct outer sphere $S_H2$ mechanism (Figure 2a).[20] This mechanism has been demonstrated outside the cellular environment by using stoichiometric cobalamin complexes. Thermal decomposition generates a 2-bisethoxycarbonylpropyl radical, which undergoes $S_H2$ with thermostable methylcobalamin to furnish the methylated product (Figure 2b).[21] Beyond cobalamins, $S_H2$ has been studied extensively in the context of carbon−heteroatom bond formation,[22,23] but until recently its application in catalytic C($sp^3$)−C($sp^3$) cross-coupling had been "seldom postulated, rarely discussed, and frequently discarded as improbable,"[24] and remained largely unexplored.[25]

Drawing inspiration from nature, we hypothesized that an $S_H2$-based platform could overcome several challenges plaguing radical C($sp^3$)−C($sp^3$) cross-coupling (Figure 2c). In an $S_H2$ mechanism, the capture of alkyl radicals by a metal catalyst is influenced by the degree of substitution or steric hindrance. More substituted alkyl radicals (2° and 3°) tend to bind weakly and reversibly to the metal, allowing less substituted 1° radicals to preferentially form stronger metal−carbon bonds, generating a more persistent metal−alkyl complex while leaving the more substituted radicals unbound.[26] This phenomenon leads to a "radical sorting effect," effectively partitioning alkyl radicals based on their degree of substitution. Additionally, when C($sp^3$)−C($sp^3$) bond formation occurs via an $S_H2$ pathway, the more substituted radical, being more electron-rich and nucleophilic, is better positioned to engage in nucleophilic attack of the electrophilic 1° alkyl−metal complex, adding a constructive electronic dimension to the sorting mechanism.[27] Consequently, an outer sphere C($sp^3$)−C($sp^3$) bond-forming process offers two key advantages: (1) improved cross-selectivity for any sterically differentiated coupling partners and (2) suppression of unproductive side reactions, including $\beta$-hydride elimination,


https://doi.org/10.1021/jacs.5c07367
J. Am. Chem. Soc. 2025, 147, 23351−23366

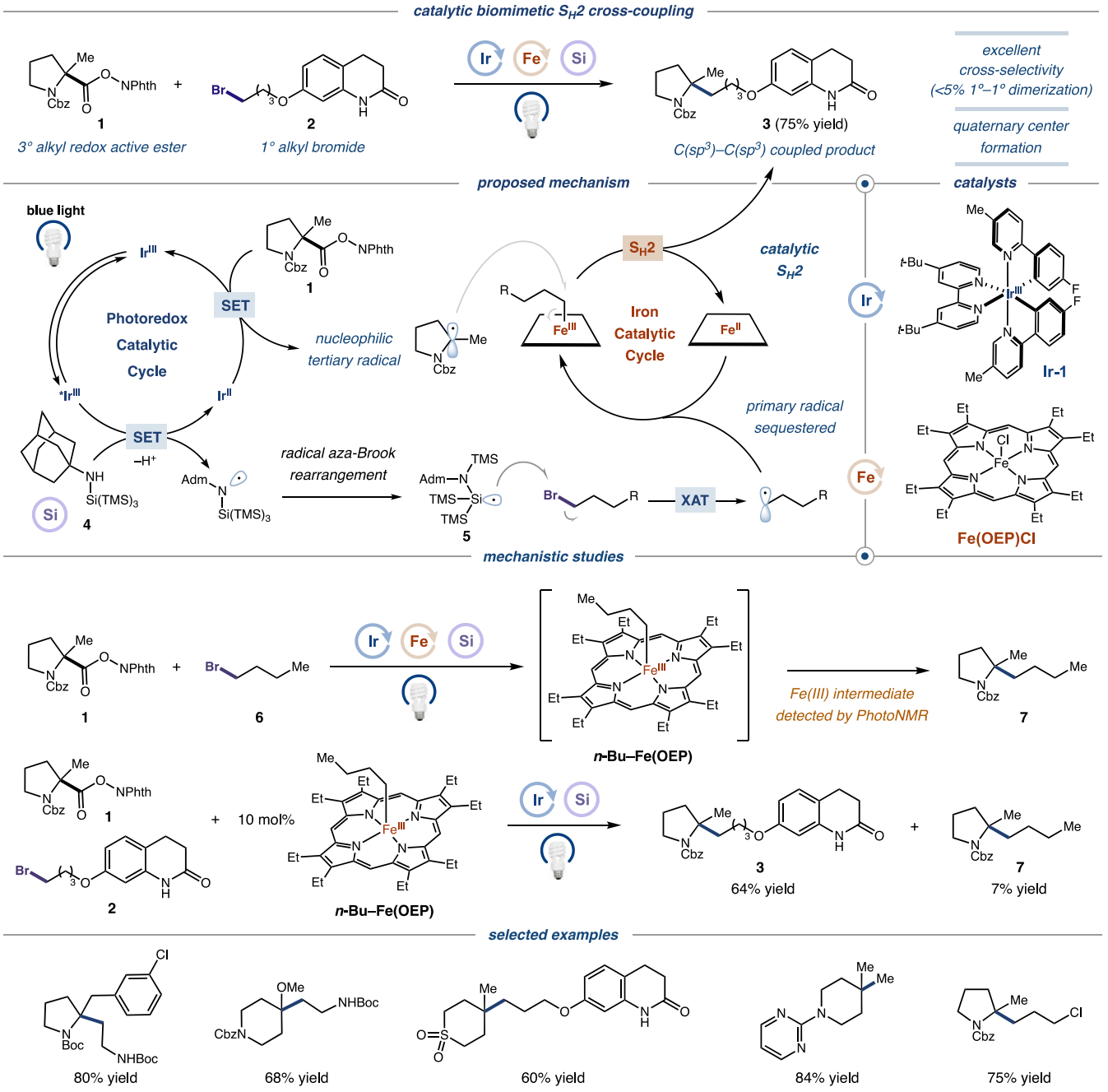


**Figure 3.** Dual iron and photoredox-catalyzed biomimetic $S_H2$ $C(sp^3)$–$C(sp^3)$ cross-coupling of alkyl redox active esters (RAEs) with 1° alkyl bromides for efficient quaternary carbon center (QCC) formation.

a particular challenge in QCC formation, as the mechanism does not require binding of hindered 3° radicals.

In 2021, our laboratory introduced the concept of $S_H2$ radical sorting catalysis in the context of an iron porphyrin-catalyzed $C(sp^3)$–$C(sp^3)$ cross-coupling of redox-active esters (RAEs) and 1° alkyl bromides that achieves efficient QCC formation under visible light photoredox (vide infra).[24a] In the subsequent years, our group and others have developed a series of powerful new $S_H2$ radical sorting $C(sp^3)$–$C(sp^3)$ cross-coupling methods. A recent review[28] has documented progress in this field, particularly focusing on transition-metal-catalyzed $S_H2$ reactions. In this perspective, we aim to provide a comprehensive analysis of key developments in $S_H2$ radical $C(sp^3)$–$C(sp^3)$ cross-coupling from 2021 to 2024, with an emphasis on iron, nickel, and cobalt catalysis, while highlighting the value of the radical sorting effect and its role in QCC formation,[29] along with emerging strategies for a highly heteroselective single functional group cross-coupling. Additionally, we discuss new opportunities for $C(sp^3)$–$C(sp^3)$ bond formation and QCC construction in the context of $S_H2$-mediated alkene functionalizations with readily available feedstock partners.

## 2. DUAL IRON AND PHOTOREDOX-CATALYZED $C(SP^3)$–$C(SP^3)$ CROSS-COUPLING: THE ADVENT OF $S_H2$ RADICAL SORTING CATALYSIS

A key objective in our laboratory is the development of metallaphotoredox platforms that employ abundant and



https://doi.org/10.1021/jacs.5c07367
J. Am. Chem. Soc. 2025, 147, 23351–23366

diverse C(sp$^3$)-rich native functionalities for radical C(sp$^3$)−C(sp$^3$) cross-coupling reactions.[14] To this end, we have introduced numerous strategies, including cross-electrophile coupling[30] and C−H functionalization.[31] However, our efforts to achieve coupling via traditional inner sphere bond-forming mechanisms were beset by moderate selectivity for cross-coupling over homocoupling and inefficient formation of QCCs. Inspired by enzymatic $S_H2$ C(sp$^3$)−C(sp$^3$) bond-forming processes, we questioned whether this unique outer sphere mechanistic platform could be adopted in a laboratory setting to achieve the proposed radical sorting effect. We noted that both cobalt and iron porphyrins are well-known analogues that mimic the reactivity of cobalamin.[32,33] Realization of catalytic $S_H2$ C(sp$^3$)−C(sp$^3$) cross-coupling with these catalyst scaffolds could greatly expand our fundamental understanding of the reactivities of metal−alkyl complexes and unveil a new general strategy for radical C(sp$^3$)−C(sp$^3$) cross-coupling.

To this end, we identified an iron porphyrin scaffold, Fe(OEP)Cl [OEP = 2,3,7,8,12,13,17,18-octaethyl-21*H*,23*H*-porphine], as a uniquely effective catalyst to accomplish the biomimetic $S_H2$ cross-coupling of RAEs with 1° alkyl bromides under photoredox conditions (Figure 3).[25] Under blue light irradiation, an excited-state iridium photocatalyst (**Ir-1**) undergoes single-electron transfer (SET) with the amino-supersilane reagent, $(TMS)_3SiNHAdm$ (**4**), to generate, upon radical aza-Brook rearrangement, a reactive silyl radical (**5**) and a reduced Ir(II) complex (Figure 3, top left). Facile bromine atom abstraction from 1° alkyl bromide (**2**) by **5** forms the 1° alkyl radical. Concurrently, the Ir(II) complex can reduce the RAE (**1**) via SET to afford, upon the loss of $CO_2$ and phthalimide, a nucleophilic 3° radical and the regenerated ground-state **Ir-1**. In the iron catalytic cycle, the less sterically hindered 1° alkyl radical is expected to be favorably sequestered by Fe(OEP) to form a moderately persistent Fe(III)−alkyl intermediate, leaving the more nucleophilic 3° alkyl radical free to engage in $S_H2$ C(sp$^3$)−C(sp$^3$) bond formation and construct the QCC (Figure 3, top right). Importantly, selective capture of the less hindered 1° radical also decreases its effective concentration, limiting the potential for free radical side reactions, such as dimerization. Moreover, the less nucleophilic nature of the 1° radical suppresses $S_H2$-mediated homocoupling. Conversely, the steric encumbrance of the 3° radical serves to discourage its effective binding to the metal center, minimize free radical dimerization, and reduce the likelihood of a bond-forming $S_H2$ event, even if the 3° metal−alkyl intermediate does form. Indeed, the desired cross-coupled product **3** is isolated in 75% yield with minimal radical homodimerization, demonstrating a strong radical sorting effect, as hypothesized. Key mechanistic studies, including photoNMR (Figure 3, middle) and light-free stoichiometric studies, support an $S_H2$ mechanism in the C(sp$^3$)−C(sp$^3$) bond-forming step. Notably, the square planar geometry of the porphyrin ligand scaffold rules out the possibility of the *cis*-coordination of both alkyl fragments, which would be required for an inner sphere reductive elimination pathway. Additionally, Fe(III)-alkyl complex ***n*-Bu−Fe(OEP)** was found to be an active catalyst that preserves the reactivity of the free Fe(II) complex, supporting the catalytic relevance of the Fe(III)−1° alkyl complex and the nucleophilicity of the 3° radical. The formation of alkylated product **7** further supports the participation of the Fe(III)−alkyl complex in the cross-coupling event. Ultimately, a wide variety of RAEs and 1° alkyl bromides could be employed as modular coupling fragments to form diverse C(sp$^3$)-rich quaternary carbon scaffolds efficiently and in good yields (Figure 3, bottom). This seminal work established $S_H2$ radical sorting catalysis as a promising new platform to achieve highly cross-selective C(sp$^3$)−C(sp$^3$) coupling reactions and challenging QCC constructions and has inspired multiple ongoing efforts to expand this concept to different transition-metal catalysts and new classes of coupling partners.

## 3. IRON-CATALYZED $S_H2$ C(SP$^3$)−C(SP$^3$) CROSS-COUPLING AND QCC FORMATION

**3.1. Cross-Coupling of 3° Alcohols with 1° Alkyl Bromides.** Having established Fe(OEP)Cl as an effective $S_H2$ catalyst scaffold, we sought to expand access to QCCs through an iron porphyrin-catalyzed photoredox cross-coupling of 3° alcohols with 1° alkyl bromides (Figure 4).[34] The alcohol

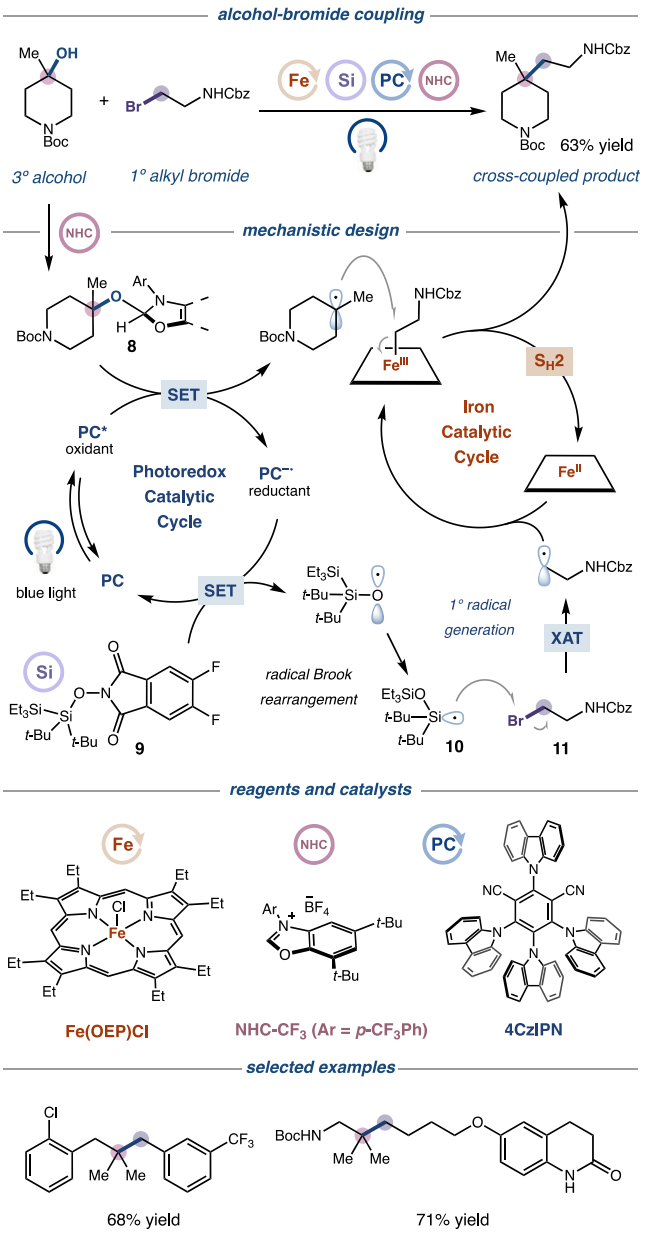


**Figure 4.** Metallaphotoredox-catalyzed $S_H2$ C(sp$^3$)−C(sp$^3$) cross-coupling of 3° alcohols with 1° alkyl bromides.



https://doi.org/10.1021/jacs.5c07367
J. Am. Chem. Soc. 2025, 147, 23351−23366

coupling partner was condensed with a bench-stable benzoxazolium salt (**NHC−$CF_3$**) previously developed in our lab that condenses with 3° alcohols under mild conditions.[35] The resulting NHC-alcohol adduct **8** can be oxidatively activated via excited photocatalyst (4CzIPN)-induced SET to generate the 3° alkyl radical upon sequential deprotonation and $\beta$-scission. To render the transformation redox neutral, the novel reductive halogen-atom transfer (XAT) silane reagent **9** was developed. The reduction of **9** by the reduced-state photocatalyst via SET induces a N−O bond cleavage and generates the reactive silyl radical **10** upon the extrusion of 4,5-difluorophthalimide and a subsequent radical Brook rearrangement. A rapid XAT event between **10** and 1° alkyl bromide **11** yielded the 1° alkyl radical. At this stage, the 1° and 3° alkyl radicals can be effectively sorted by the iron porphyrin catalyst to afford the highly congested QCC product via $S_H2$. This cross-coupling proceeds with high yields (up to 83%) and excellent functional group tolerance, while maintaining high cross-selectivity over radical homocoupling. Notably, the system is compatible with substrates containing aryl chlorides, which are susceptible to oxidative addition under traditional cross-coupling conditions involving low-valent metal catalysts, highlighting another advantage of the distinct $S_H2$ elementary step. Furthermore, this modular fragment coupling strategy was employed for the expedited synthesis of bioactive molecules, achieving the facile construction of otherwise challenging QCCs.

**3.2. Cross-Electrophile Coupling of 3° Alkyl Bromides with 1° Alkyl Electrophiles.** More recently, our laboratory demonstrated that 3° alkyl bromides serve as viable coupling partners for iron porphyrin-catalyzed $S_H2$ QCC formation in the context of a photoredox-mediated cross-electrophile coupling (Figure 5).[36] In the presence of 3° and 1° alkyl bromide substrates, the silyl radical generated from Ir(III)* photocatalyst-mediated single-electron oxidation of amino-supersilane (**4**) selectively undergoes XAT with the 3° alkyl bromide to form radical **12**. Concurrently, the reduced Ir(II) photocatalyst performs a single-electron reduction of Fe(II)(OEP) to afford a highly nucleophilic Fe(I)(OEP) species, which is poised to undergo a sterically favorable $S_N2$ reaction with the 1° alkyl bromide, yielding the Fe(III)−alkyl intermediate **13**. $S_H2$-mediated C($sp^3$)−C($sp^3$) bond formation between **12** and **13** forges the desired QCC in high yields. Owing to the $S_N2$ activation mode for 1° alkyl fragments, this new strategy expanded the scope of 1° alkyl electrophiles beyond alkyl halides, enabling the adoption of 1° alkyl sulfonates derived from abundant alcohols as viable coupling partners and further enhancing the utility of this transformation.

**3.3. Enantioselective Cross-Coupling of $\beta$-Keto Esters/Amides with 1° Alkyl RAEs.** When merged with organophotoredox catalysis, the $S_H2$ cross-coupling platform can be extended to enantioselective QCC formation. In 2024, Yang and co-workers invoked $S_H2$ as an elementary step in the enantioselective cross-coupling of $\beta$-keto esters or amides with unactivated 1° alkyl RAEs to construct enantioenriched QCCs via a cooperative photoredox/iron porphyrin/chiral amine triple catalysis (Figure 6).[37] First, the $\beta$-keto ester or amide substrate condenses with a primary amine organocatalyst **14** to form chiral enamine **15**, which can be readily activated by an excited Ir(III) photocatalyst (**Ir-2** = Ir(dF($CF_3$)ppy)$_2$(dtbbpy)$PF_6$ [dF($CF_3$)ppy = 2-(2,4-difluorophenyl)-5-trifluoromethylpyridine]) via oxidative SET to generate a

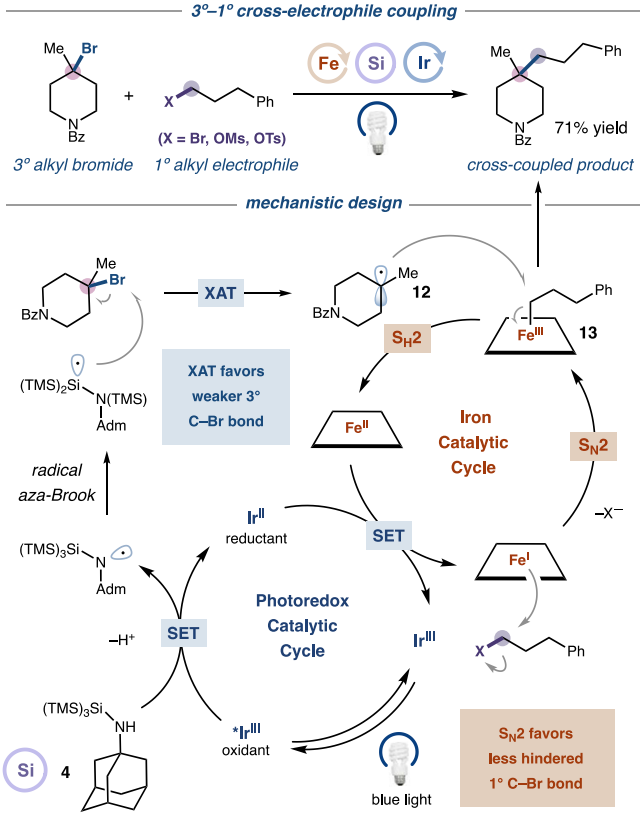


**Figure 5.** Metallaphotoredox-catalyzed 3°−1° C($sp^3$)−C($sp^3$) cross-electrophile coupling via $S_H2$.

sterically hindered 3° radical **16**. The resulting Ir(II) complex reduces the RAE and furnishes 1° alkyl radical **17** through a N−O bond cleavage and decarboxylation. At this point, the Fe(OEP) catalyst selectively captures the less substituted alkyl radical, **17**, to form the Fe(III)−alkyl intermediate, which is subsequently intercepted by the chiral 3° radical **16** to deliver the enantioenriched QCC product **18** via $S_H2$ in excellent enantiomeric excess (ee). The chiral amine catalyst is regenerated upon hydrolysis. This transformation works on a gram scale without the loss of yield or ee and can be used for the construction of a variety of cyclic and acyclic QCCs, highlighting the extraordinary cooperative ability of $S_H2$ radical sorting and organocatalysis to enable challenging asymmetric transformations.

**3.4. Single Functional Group Cross-Coupling of RAEs.** The cross-selectivity of $S_H2$ radical sorting catalysis makes it amenable to single functional group cross-coupling, wherein two distinct fragments bearing the same functional group are concurrently activated via a single activation mode and subsequently coupled, without the requirement that one fragment is used in large excess to ensure statistical cross-selectivity.[38] In 2024, the Shenvi and Baran groups developed a highly cross-selective decarboxylative coupling of aliphatic RAEs that achieves efficient QCC formation via iron porphyrin-mediated $S_H2$ radical sorting catalysis (Figure 7).[39] Notably, in addition to the previously established Fe(OEP)Cl scaffold, the researchers report that Fe(TPP)Cl [TPP = 5,10,15,20-tetraphenyl-21*H*,23*H*-porphine] serves as an alternative iron porphyrin catalyst competent in promoting $S_H2$ reactivity. Fe(III) can be reduced by the zinc metal to Fe(II), which in turn reduces the RAEs to generate the mixture of


https://doi.org/10.1021/jacs.5c07367
J. Am. Chem. Soc. 2025, 147, 23351−23366

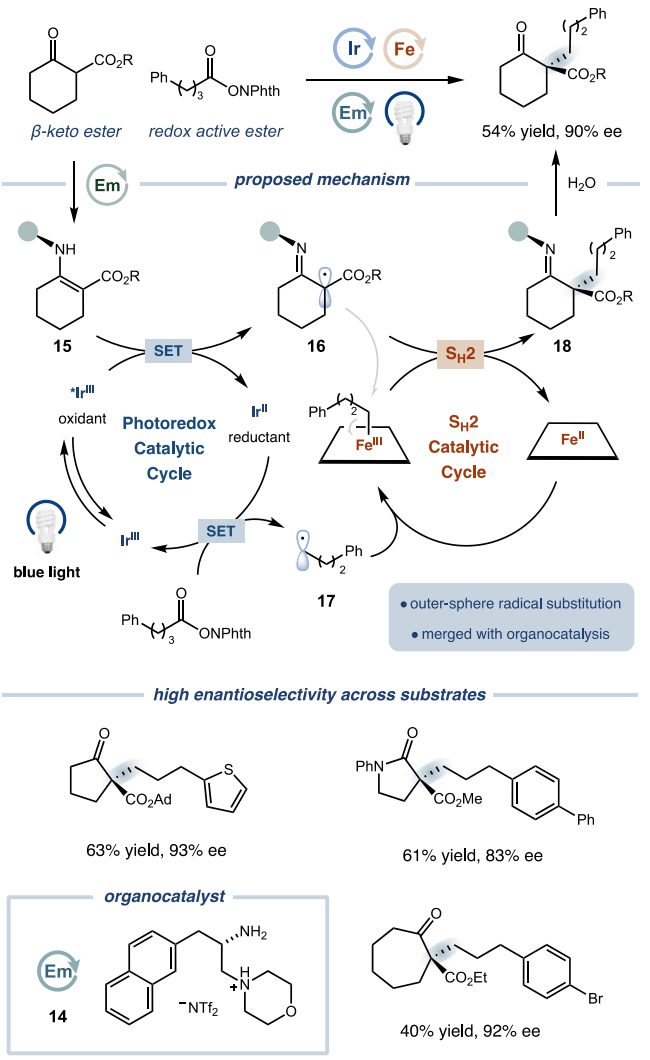


**Figure 6.** Photoredox/iron porphyrin/chiral amine triple catalytic enantioselective C(sp$^3$)−C(sp$^3$) cross-coupling of β-keto esters or amides with unactivated 1° alkyl RAEs via S$_H$2.

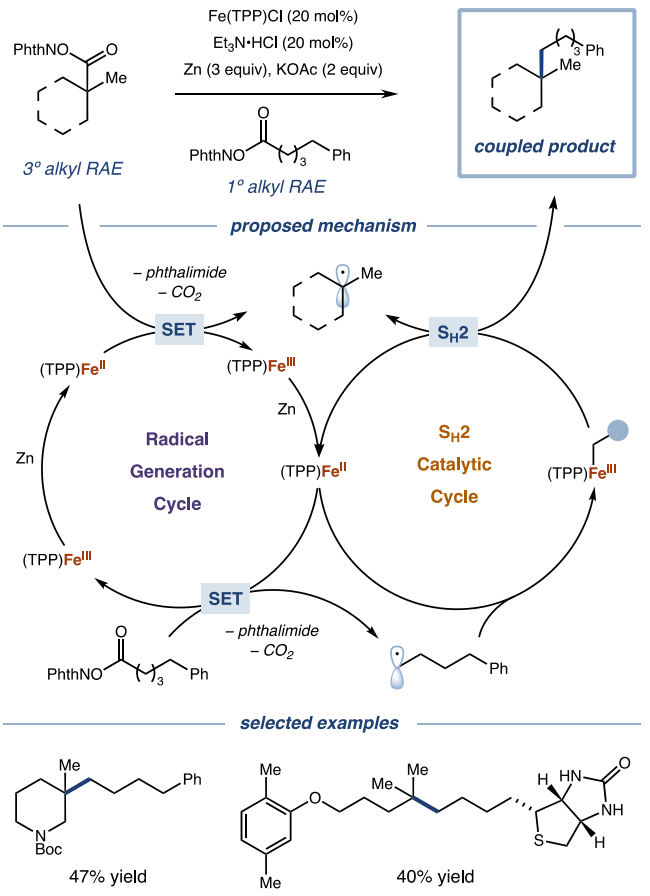


**Figure 7.** Iron porphyrin-catalyzed decarboxylative S$_H$2 C(sp$^3$)−C(sp$^3$) cross-coupling of RAEs.

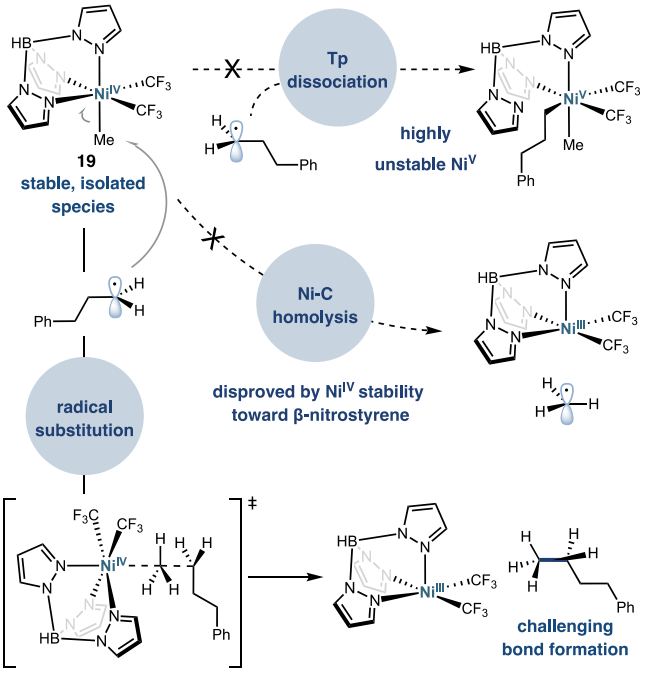


**Figure 8.** Sanford's seminal discovery of a (Tp)Ni(IV)−methyl complex that mediates C(sp$^3$)−C(sp$^3$) bond formation through the S$_H$2 mechanism.

alkyl radicals, possibly via an electron donor−acceptor (EDA) complex-mediated SET event (Figure 7, middle left).[40] Subsequently, the Fe(TPP) scaffold also serves as an efficient radical sorting platform to enable a highly cross-selective S$_H$2 C(sp$^3$)−C(sp$^3$) bond-forming event (Figure 7, middle right). This streamlined reaction protocol demonstrated the modular assembly of QCCs from commercially available building blocks, further revealing the revolutionary potential of S$_H$2 radical sorting catalysis to simplify the complex molecule synthesis and modernize retrosynthetic strategies.[41]

## 4. NICKEL-CATALYZED S$_H$2 C(SP$^3$)−C(SP$^3$) CROSS-COUPLING AND QCC FORMATION

Nickel, a highly versatile first-row transition metal, plays a pivotal role in modern cross-coupling reactions[5] and has demonstrated a unique ability to mediate C(sp$^3$)−C(sp$^3$) bond formation via the S$_H$2 pathway. Seminal studies by Sanford and co-workers in 2019 established that high-valent Ni(IV)−alkyl complexes, supported by a distinctive scorpionate tris-(pyrazolyl)borate (Tp) ligand, can facilitate S$_H$2-mediated C(sp$^3$)−C(sp$^3$) bond formation with alkyl radicals (Figure 8).[42] In this work, the addition of a methyl radical to the Ni(Tp)(CF$_3$)$_2$ complex resulted in the formation of the model Ni(IV)−methyl species **19**, which displayed remarkable



https://doi.org/10.1021/jacs.5c07367
J. Am. Chem. Soc. 2025, 147, 23351−23366

thermal stability while rapidly reacting with alkyl radicals generated from the thermolysis of acylperoxides to form C($sp^3$)−methyl bonds. The possibility of an inner sphere reductive elimination pathway was considered unlikely due to an elusive Ni(V) oxidation state, and homolysis of the Ni(IV)−methyl bond was ruled out due to the thermostability of the complex. The most plausible mechanism is the nucleophilic attack of the Ni(IV)−methyl complex by the alkyl radicals, a process that resembles the $S_H2$ reactivity of methylcobalamin in biological systems. This landmark discovery opened new avenues for $S_H2$ catalysis in previously elusive nickel-catalyzed C($sp^3$)−C($sp^3$) cross-coupling and has significant implications for overcoming the limitations of traditional cross-coupling mechanisms, particularly in the formation of QCCs.

**4.1. Single Functional Group Cross-Coupling of Aliphatic Carboxylic Acids Enabled by a Ni(II) Scorpionate Catalyst.** Inspired by the pioneering work from the Sanford group, in 2022 our laboratory established the first proof of concept for Ni-mediated $S_H2$ radical sorting catalysis in the context of the double decarboxylative cross-coupling of aliphatic acids (Figure 9).[43] Aliphatic carboxylic acids with distinct $\alpha$-substitution are activated in situ by iodosomesitylene to form I(III) carboxylates. Under UV or blue light irradiation with thioxanthone (TXO) or 4CzIPN, respectively, as the photosensitizer, I−O bond homolysis followed by $CO_2$ extrusion generates the free alkyl radicals. A unique Ni(II) catalyst, supported by a sterically bulky tris(3,5-dimethylpyrazolyl)borate (Tp*) ligand, preferentially sequesters methyl and small 1° alkyl radicals, forming more stable (Tp*)Ni(III)−alkyl complexes, as evidenced by photoEPR experiments. More substituted radicals, such as 2° and 3° radicals, undergo $S_H2$ substitution with the (Tp*)Ni(III)−alkyl complex, yielding the desired cross-coupled product and regenerating the Ni(II) catalyst. Remarkably, this transformation exhibits a high reaction efficiency and cross-selectivity, particularly for C($sp^3$)−methyl couplings, highlighting the ability of the specialized nickel scorpionate scaffold to engage in the $S_H2$ radical sorting pathway. Consequently, this approach enables the efficient formation of a broad range of high-value C($sp^3$)−methyl bonds, especially in the context of QCCs, offering a novel solution to a long-standing synthetic challenge using abundant starting materials. This work also represents a key demonstration of the ability of $S_H2$ radical sorting catalysis to enable highly cross-selective single functional group coupling reactions.

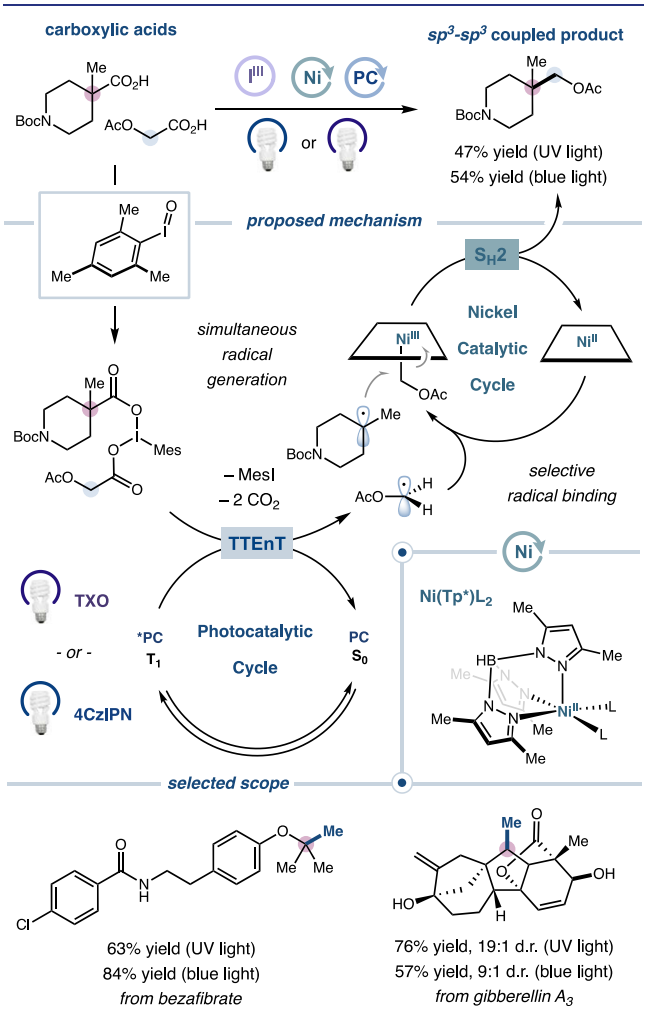


**Figure 9.** Photoredox decarboxylative $S_H2$ C($sp^3$)−C($sp^3$) cross-coupling of aliphatic acids enabled by a (Tp*)Ni(II) complex.

**4.2. Late-Stage C($sp^3$)−H Methylation of Drug Molecules.** The "magic methyl effect" refers to the substantial improvement in pharmaceutical properties that may arise when a methyl group is strategically introduced to a small molecule drug candidate and is particularly pronounced in molecules bearing saturated heterocyclic cores.[44] Despite the value of this motif, the direct introduction of methyl groups to lead compounds or drug candidates via late-stage functionalization remains a significant challenge.[45,46] Inspired by the ability of (Tp*)Ni(II) complexes to promote C($sp^3$)−methylation in radical cross-couplings, we sought to develop a nickel-catalyzed platform for the C($sp^3$)−H methylation of drug molecules. In 2023, we reported a novel late-stage C($sp^3$)−H methylation protocol that merges photoinduced decatungstate-mediated selective hydrogen atom-transfer (HAT) catalysis with nickel $S_H2$ radical sorting catalysis (Figure 10).[47] Photoexcitation of decatungstate anion $[W_{10}O_{32}]^{4-}$ under 365 nm LED irradiation induces highly selective hydrogen atom abstraction (HAA) of the hydridic $\alpha$-C−H bonds present in a drug-like saturated heterocyclic substrate, generating a nucleophilic $\alpha$-heteroatom carbon-centered radical, **20**. Meanwhile, RAE, derived from acetic acid, undergoes reduction via SET to form the methyl radical upon the N−O bond cleavage and decarboxylation. The methyl radical preferentially binds to the (Tp*)Ni(II) complex and, following $S_H2$ substitution, the desired C($sp^3$)−methyl bond is obtained. This late-stage C($sp^3$)−H methylation protocol allows for rapid access to methylated analogues of pharmaceutically relevant heterocyclic scaffolds as well as FDA-approved drug molecules, significantly expediting the exploration of the "magic methyl effect" by removing the burden of the lengthy de novo synthesis.

**4.3. Cross-Coupling of Aliphatic Carboxylic Acids with Alcohols Using Ni(II) Diketonate Catalysts.** Recently, computational studies have suggested that diketonate ligands promote Ni-catalyzed radical C($sp^2$)−C($sp^3$) cross-couplings to construct QCCs via an outer sphere bond-forming mechanism.[48] Indeed, in 2022, our laboratory demonstrated that nickel diketonate complexes are highly effective catalyst scaffolds capable of facilitating $S_H2$ radical sorting through the nontraditional C($sp^3$)−C($sp^3$) fragment coupling of aliphatic carboxylic acids and alcohols under photoredox catalysis (Figure 11).[49] Carboxylic acids and


https://doi.org/10.1021/jacs.5c07367
J. Am. Chem. Soc. 2025, 147, 23351−23366

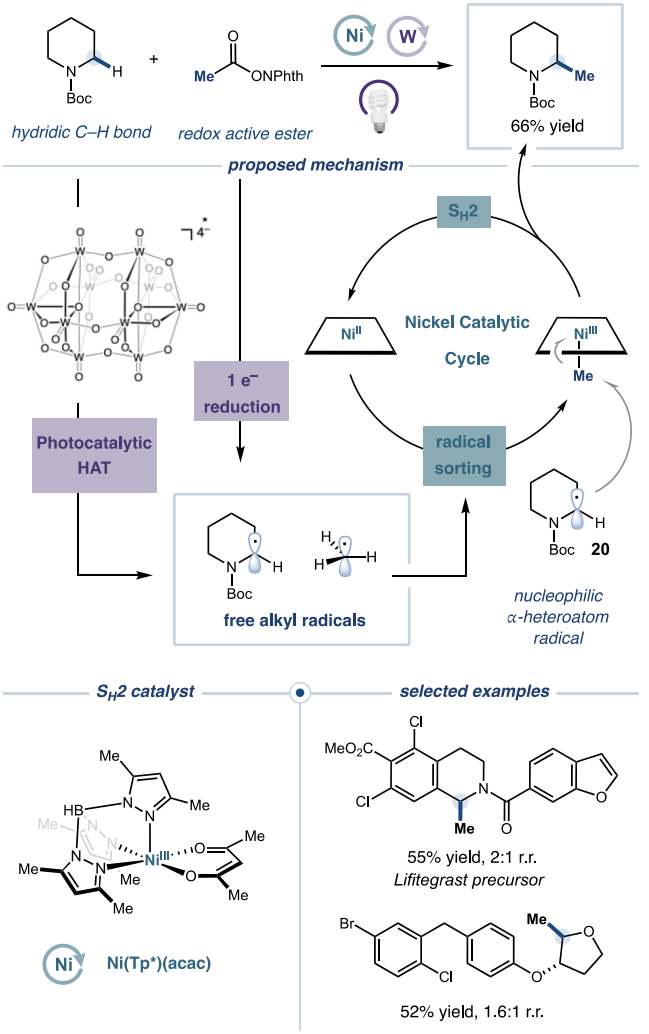


**Figure 10.** Late-stage C($sp^3$)−H methylation of drug molecules via a (Tp*)Ni(II)-mediated $S_H2$ pathway.

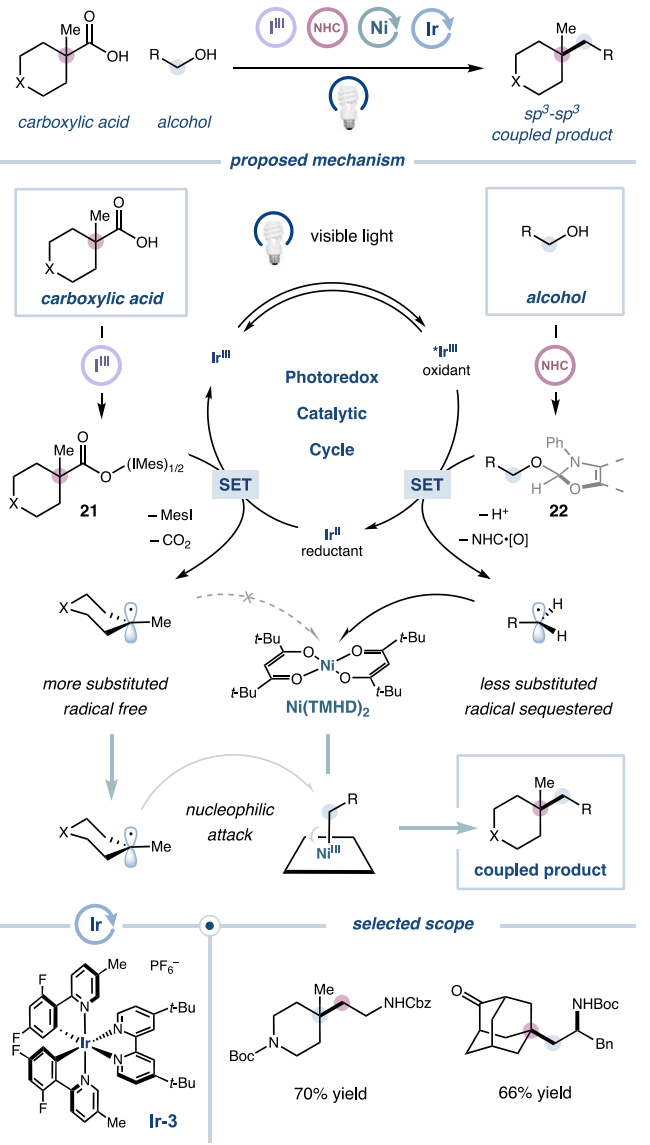


**Figure 11.** Photoredox-enabled nontraditional C($sp^3$)−C($sp^3$) fragment coupling of aliphatic carboxylic acids with alcohols via nickel diketonate-mediated $S_H2$ radical sorting catalysis.

alcohols are independently activated by mixing them with iodomesitylene diacetate and an NHC activator, respectively. The resulting iodonium dicarboxylate (**21**) and NHC-alcohol adduct (**22**) engage in SET processes with **Ir-3** as the photocatalyst to afford the corresponding decarboxylated and deoxygenated alkyl radicals via a redox-neutral photoredox cycle (Figure 11, middle). Our optimal nickel catalyst, Ni(TMHD)$_2$ [TMHD = 2,2,6,6-tetramethyl-3,5-heptanedionate], selectively cross-couples these two distinct alkyl radicals following $S_H2$ radical sorting principles. Of note, this platform displays excellent reactivity and enhanced selectivity when $\beta$-amino substrates are utilized as the less substituted coupling partner, presumably due to the stabilization of the Ni(III)−alkyl intermediates via chelation. Consequently, a wide variety of aliphatic alcohols and carboxylic acids were successfully employed to facilitate cross-selective nontraditional fragment couplings and effective QCC construction.

**4.4. Single Functional Group Cross-Coupling of Alcohols.** We previously demonstrated the unparalleled ability of aliphatic alcohols to serve as versatile, abundant, and diverse radical precursors in C($sp^3$)−C($sp^3$) cross-coupling reactions. In 2024, our laboratory described the use of radical sorting principles to achieve the single functional group cross-coupling of aliphatic alcohols to unlock access to an unprecedented C($sp^3$)-rich chemical space (Figure 12).[50] Aliphatic alcohols bearing distinct $\alpha$-substitution patterns were simultaneously activated in situ via condensation with NHC salts under mildly basic conditions to form a mixture of NHC−alcohol adducts. Under photoredox conditions, these adducts undergo deoxygenative radical generation, and the resulting radical species participate in the nickel-mediated $S_H2$ radical sorting to form the desired C($sp^3$)−C($sp^3$) bond with a high degree of cross-selectivity.

We observed that benzoyl peroxide serves as a viable external oxidant, allowing for the turnover of the photoredox cycle. Ultimately, five distinct classes of C($sp^3$)−C($sp^3$) bond-forming reactions, especially in the context of QCC formation, could be achieved in high efficiency from these abundant and accessible alkyl alcohol precursors. The excellent cross-selectivity resulting from radical sorting was particularly highlighted in the case of 1° methylation, where we observed a high ratio of cross-coupling compared with 1° dimerization. Notably, in situ-generated nickel scorpionate (Tp*)Ni(acac)


https://doi.org/10.1021/jacs.5c07367
J. Am. Chem. Soc. 2025, 147, 23351−23366

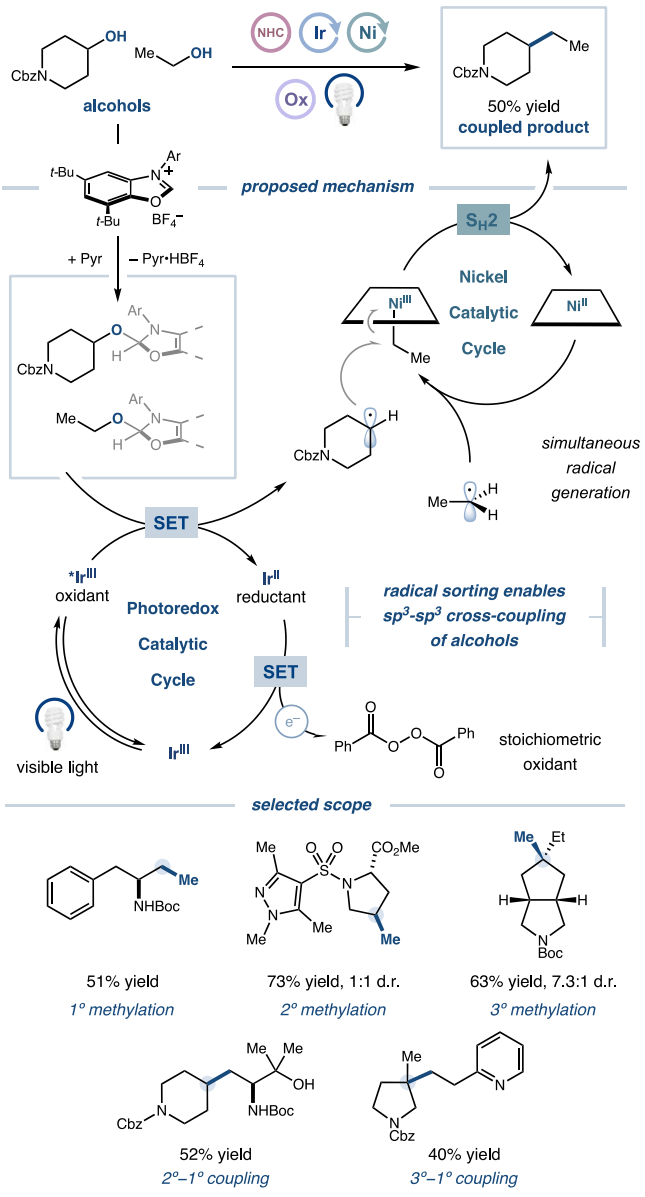


**Figure 12.** Photoredox-catalyzed single functional group $C(sp^3)$–$C(sp^3)$ cross-coupling of alcohols enabled by nickel $S_H2$ radical sorting.

demonstrated a superior catalytic performance in the context of 3° methylation, whereas diketonate catalyst $Ni(acac)_2$ was generally successful for other types of cross-couplings. This simple, user-friendly, and open-to-air reaction setup for alcohol–alcohol cross-coupling is expected to have immediate implications in applied chemical sciences.

## 5. RADICAL FUNCTIONALIZATION OF ALKENES: NEW OPPORTUNITIES FOR $S_H2$ $C(SP^3)$–$C(SP^3)$ CROSS-COUPLING AND QCC FORMATION

Previous examples have highlighted the ability of $S_H2$ to enable highly cross-selective fragment couplings utilizing a variety of common $C(sp^3)$ functionalities as radical precursors. Alkenes, another important class of feedstock molecules with great structural diversity, have received increasing attention among synthetic chemists as alkyl radical precursors.[51] For instance, unactivated alkenes are well known to engage in iron-, manganese-, and cobalt-catalyzed metal-hydride hydrogen atom transfer (MHAT)[52] or react with electrophilic radicals[53] in a Markovnikov-selective fashion, thereby generating more substituted alkyl radicals for downstream cross-coupling reactions (Figure 13).[54,55] Indeed, alkenes hold the advantageous ability to couple with one or two separate radical partners in a single transformation without the preactivation steps that are required for many other functional groups. The merger of radical activation of alkenes with $S_H2$ radical sorting catalysis offers a powerful strategy to achieve regioselective olefin functionalization, thus greatly expanding the synthetic toolbox for $C(sp^3)$–$C(sp^3)$ cross-coupling and the available $C(sp^3)$-rich chemical space. In particular, this highly regioselective process offers valuable new opportunities for the direct quaternization of alkenes,[56] an appealing alternative strategy for QCC formation in $S_H2$-mediated $C(sp^3)$–$C(sp^3)$ cross-coupling.

**5.1. MHAT and Iron Porphyrin-Mediated $S_H2$.** In 2023, Shenvi and co-workers disclosed the hydrobenzylation of unactivated alkenes with 1° benzyl bromides, achieved through the integration of MHAT and $S_H2$ radical sorting catalysis, using a dual $Fe(acac)_3$/Fe(TPP)Cl catalytic system (Figure 14).[57] In the MHAT catalytic cycle, the reaction of $Fe(acac)_3$ with $PhSiH_3$ generates $Fe(acac)_2$–H, which initiates MHAT to the alkene (**23**) to afford a 3° radical and $Fe(acac)_2$. $Fe(acac)_2$–H is regenerated from the oxidation of $Fe(acac)_2$ by $O_2$ and hydride transfer. Concurrently, Fe(TPP)–H is

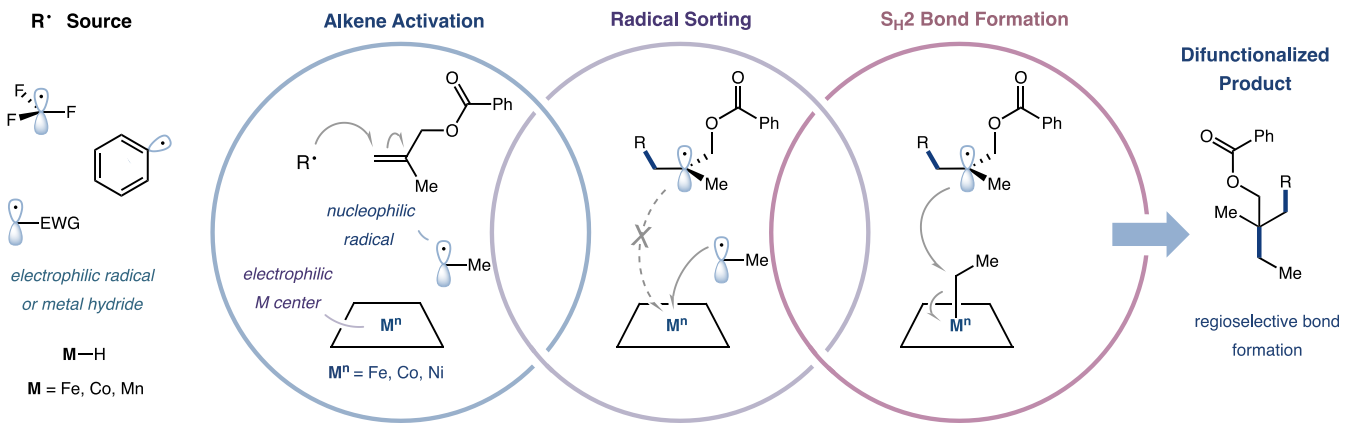


**Figure 13.** Markovnikov-selective radical generation from alkenes and its merger with $S_H2$ radical sorting catalysis for new $C(sp^3)$–$C(sp^3)$ cross-coupling development.



https://doi.org/10.1021/jacs.5c07367
J. Am. Chem. Soc. 2025, 147, 23351–23366

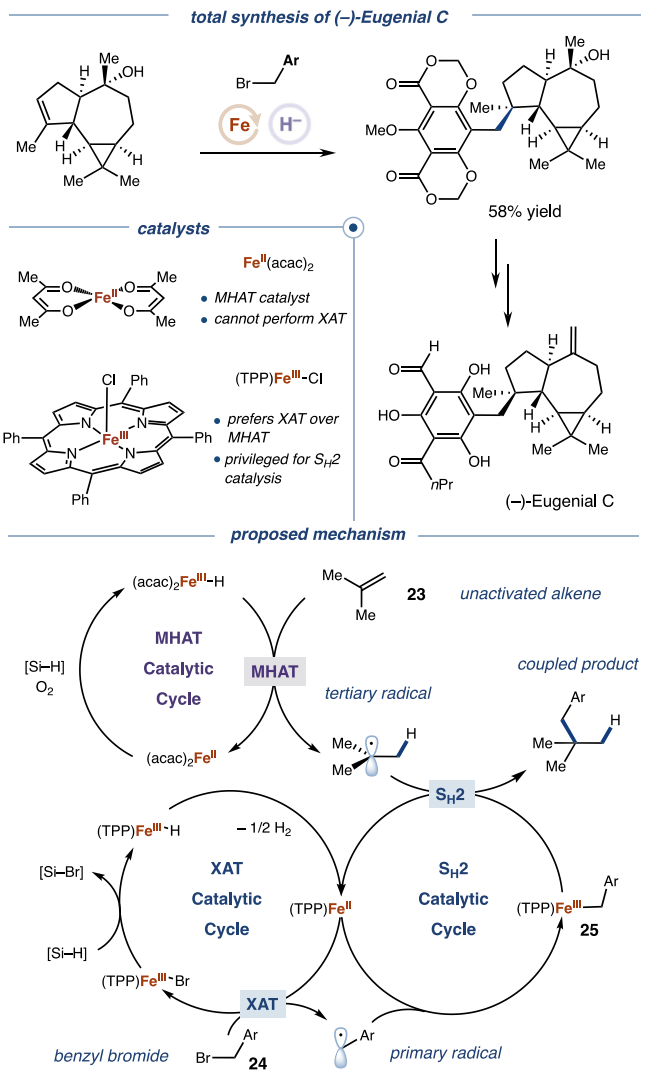


**Figure 14.** Dual iron-catalyzed hydrobenzylation of alkenes via the merger of MHAT and $S_H2$ and application to the stereoselective total synthesis of (−)-eugenial C.

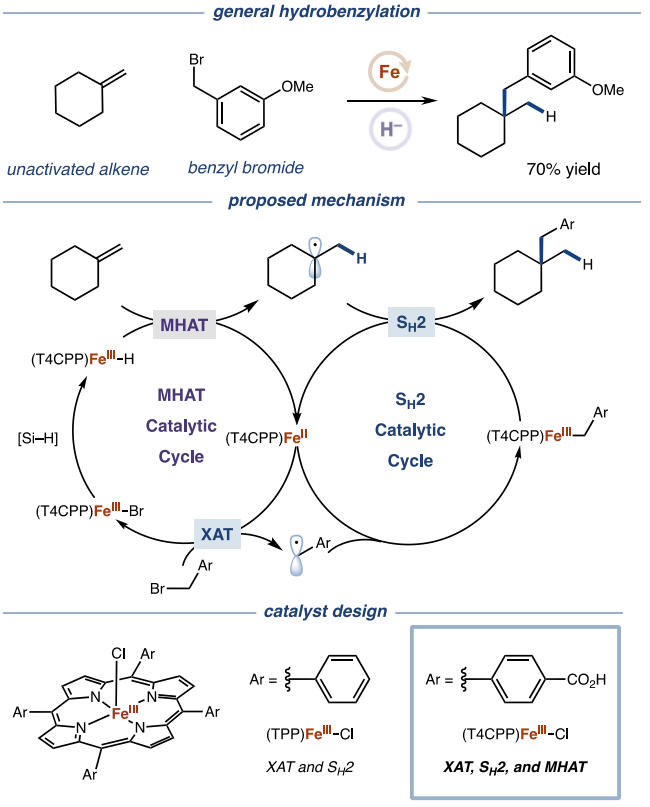


**Figure 15.** Second-generation hydrobenzylation of alkenes via a single iron porphyrin catalyst-mediated MHAT and $S_H2$.

proposed to undergo a hydrogen evolution reaction to afford Fe(TPP), which serves as an XAT platform to convert benzyl bromide **24** to a 1° radical species that is then selectively captured by another 1 equiv of Fe(TPP) to form Fe(TPP)−benzyl complex **25**. Finally, the $S_H2$ reaction between the alkene-derived 3° radical and **25** forms the QCC in the coupled product. Ultimately, a broad range of alkenes and 1° benzyl bromides could be coupled using this radical sorting platform, enabling the highly stereoselective construction of complex QCCs, including a concise synthesis of the meroterpenoid natural product (−)-eugenial C. It should be noted that $Fe(acac)_3$ was found to be necessary for a successful reaction despite the observed MHAT reactivity of Fe(TPP)−H.

Shenvi and co-workers continued to pursue the goal of developing a single iron porphyrin catalyst to simultaneously mediate the three key catalytic cycles: MHAT, XAT, and $S_H2$. In 2024, the group introduced a special iron porphyrin complex, Fe(T4CPP)Cl, that effectively mediates all the necessary elementary steps in the hydrobenzylation of alkenes with 1° benzyl bromides (Figure 15).[58] This new $S_H2$ catalytic platform enables general access to 2°−1° and 3°−1° cross-coupling products with excellent efficiency and cross-selectivity. Moreover, owing to the ability of Fe(T4CPP) to turn over by a reaction with benzyl bromide, this overall redox-neutral catalytic system no longer requires $O_2$ as an external oxidant to regenerate Fe(III) for the MHAT catalytic cycle. This second-generation platform greatly enhances the simplicity and scalability of the reaction.

Shortly after, the Shenvi and Baran laboratories reported a decarboxylative coupling of RAEs and alkenes that allows general access to QCCs via an iron porphyrin $S_H2$ radical sorting catalysis (Figure 16).[39] Fe(TPP) activates the 1° alkyl RAE via single electron reduction and also engages in a MHAT and $S_H2$ radical sorting to mediate the direct quaternization of alkenes from the corresponding radical intermediates with excellent cross-selectivity. The mild and simple reaction conditions accommodate a broad scope of coupling partners, expanding the range of 1° alkyl fragments from benzylic to unstabilized and long-chain alkyl partners.

**5.2. MHAT and Nickel-Mediated $S_H2$.** Manganese complexes can also be used to merge MHAT reactivity with the nickel $S_H2$ radical cross-coupling. In 2024, our lab developed a triple catalytic radical sorting platform for the cross-coupling of abundant alkenes and alcohols by merging metallaphotoredox and Mn-MHAT catalysis (Figure 17).[59] NHC-alcohol adduct **26**, generated in situ from the condensation of methanol with NHC salt (**NHC-1**), engages in single electron oxidation by an excited Ir(III) photocatalyst (**Ir-2**) to produce the methyl radical upon sequential deprotonation and $\beta$-scission. Meanwhile, hydride transfer from the silane to $Mn(TMHD)_3$ provides the key Mn(III)−H intermediate, which engages in Markovnikov-selective MHAT with the alkene, yielding 3° radical **27**. The resulting Mn(II)


https://doi.org/10.1021/jacs.5c07367
J. Am. Chem. Soc. 2025, 147, 23351−23366

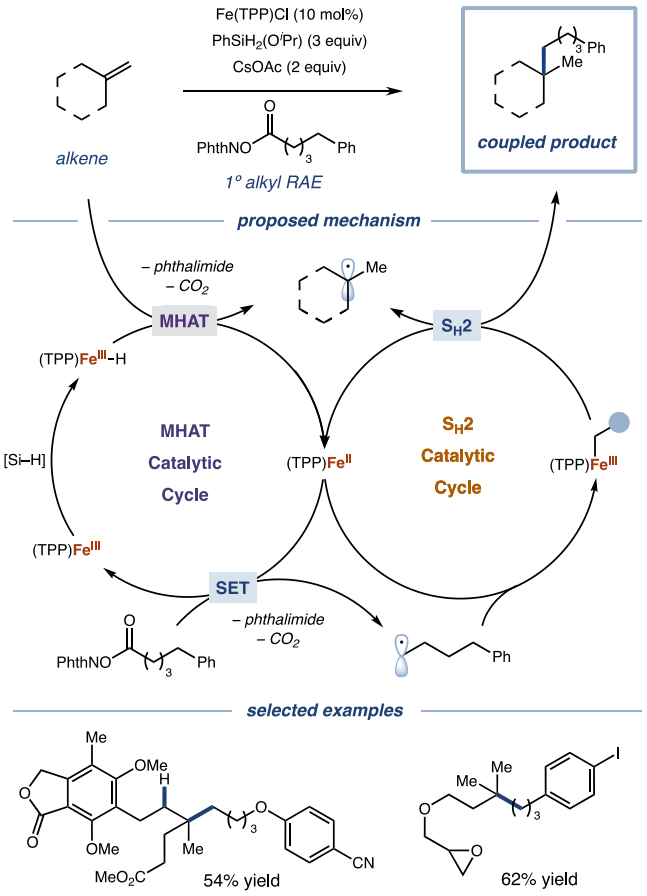


**Figure 16.** Direct quaternization of alkenes via the iron porphyrin-catalyzed MHAT/$S_H2$ cross-coupling of RAEs with alkenes.

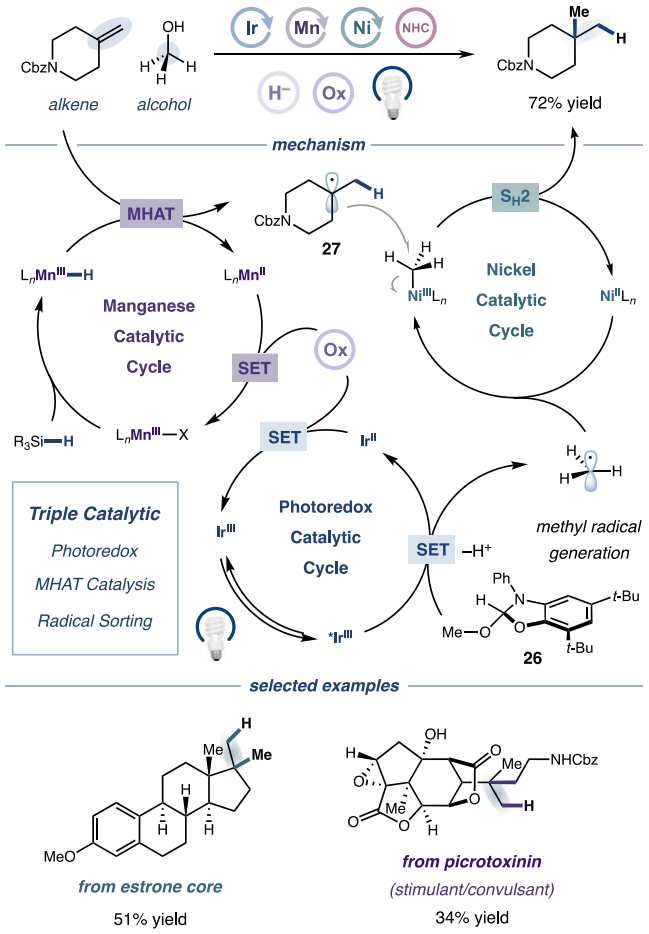


**Figure 17.** A triple catalytic $S_H2$ radical sorting-mediated $C(sp^3)$–$C(sp^3)$ cross-coupling of alkenes with alcohols.

and Ir(II) complexes are both oxidatively turned over by benzoyl peroxide as a stoichiometric oxidant. In the nickel catalytic cycle, the selective capture of the methyl radical by the (Tp*)Ni(acac) complex, followed by $S_H2$-mediated $C(sp^3)$–$C(sp^3)$ bond formation with the 3° radical, effectively delivers the hydroalkylation product with excellent cross-selectivity. This new MHAT/$S_H2$ radical sorting manifold successfully tolerates a large range of alkenes with various substitution patterns. Notably, 1° alcohols, including those bearing sensitive functional groups such as amines, proved to be suitable substrates for general hydroalkylation simply by switching to nickel diketonates as $S_H2$ catalysts. This triple catalytic methodology was also readily applied to late-stage QCC formation in complex molecules such as drug cores and natural products.

**5.3. MHAT and Cobalt-Mediated $S_H2$.** Cobalt has been shown to facilitate $C(sp^3)$–$C(sp^3)$ bond formation through the merger of MHAT and $S_H2$ radical sorting catalysis, especially in the context of QCC construction. Indeed, the Matsunaga lab integrated photoredox catalysis with MHAT and $S_H2$ using a single cobalt salen catalyst **28** to furnish QCCs from alkenes and benzyl dihydropyridines (DHPs), as depicted in Figure 18.[60] Under blue light irradiation, the excited Ir(III) complex (**Ir-4**) oxidizes benzyl DHP **29** via SET, generating a 1° benzylic radical and reduced Ir(II) following sequential deprotonation and aromatization-driven $\beta$-scission. The Co(II) salen complex **28** is then reduced by Ir(II) via SET to regenerate the photocatalyst and form Co(I), which undergoes protonation to yield the key Co(III)–H intermediate. Subsequent MHAT to an alkene substrate furnishes a 3° radical and regenerates Co(II). Finally, in the cobalt $S_H2$ cycle, the selective capture of the 1° benzylic radical by Co(II) yields the Co(III)–benzyl intermediate, which readily undergoes the $S_H2$ reaction with the 3° radical to form the QCC product. A variety of tri- and 1,1-disubstituted alkenes could be coupled with electronically differentiated benzyl DHPs in good yields.

**5.4. Electrophilic Radical Addition and Nickel-Mediated $S_H2$.** Recently, $S_H2$ radical sorting catalysis has been used to difunctionalize unactivated alkenes in three-component cross-couplings with distinct alkyl partners. This reaction framework offers new opportunities to achieve the regioselective difunctionalization of abundant alkenes to highly $C(sp^3)$-rich scaffolds and complex QCCs.

In 2024, our laboratory reported a metallaphotoredox-catalyzed dialkylation of alkenes wherein a variety of electrophilic radicals derived from $\alpha$-acyl alkyl chlorides and nucleophilic radicals from 1° alcohols are added across an alkene C=C bond with high regioselectivity (Figure 19).[61] This reaction platform entails a "triple radical sorting" mechanism involving (1) favorable electrophilic radical addition to an alkene, (2) preferential binding of a methyl or 1° radical to a nickel $S_H2$ catalyst, and (3) cross-selective $S_H2$-mediated $C(sp^3)$–$C(sp^3)$ bond formation. In the photoredox catalytic cycle, upon blue light irradiation, the in situ-generated methanol-NHC adduct engages in the reductive quenching of the excited Ir(III) photocatalyst (**Ir-2**) via SET to generate the methyl radical, which is selectively captured by the in situ


https://doi.org/10.1021/jacs.5c07367
J. Am. Chem. Soc. 2025, 147, 23351–23366

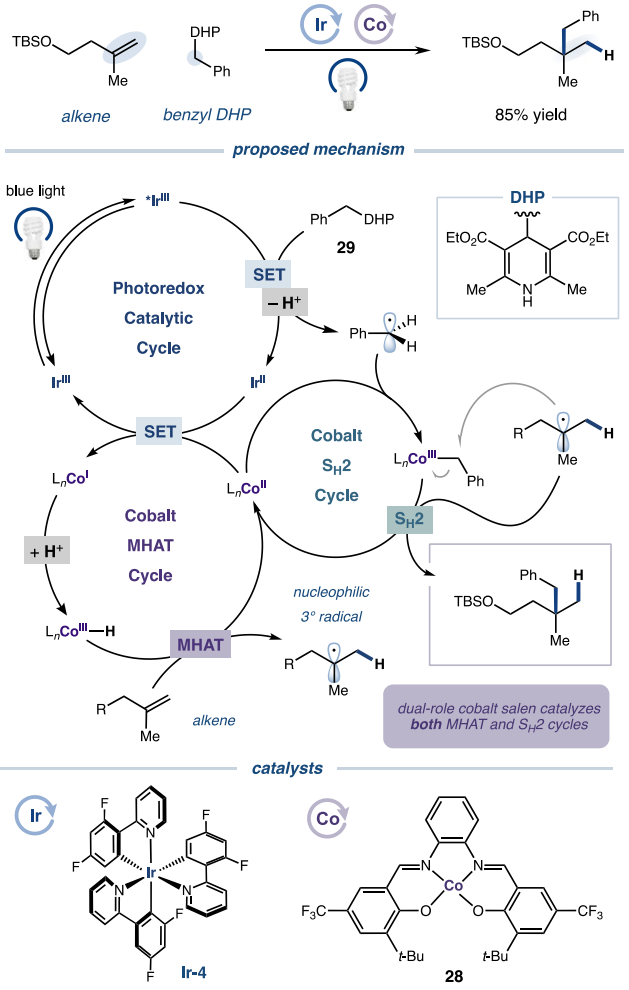


**Figure 18.** Hydroalkylation of alkenes via the cobalt salen-catalyzed MHAT/$S_H2$ cross-coupling of alkenes with DHPs.

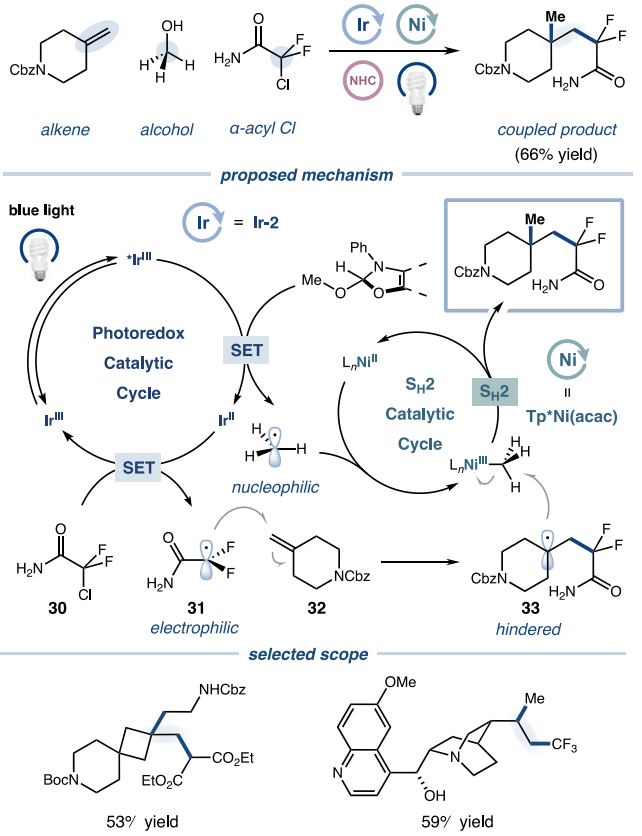


**Figure 19.** Metallaphotoredox-catalyzed regioselective dialkylation of alkenes with alkyl alcohols and α-acyl chlorides via a $S_H2$-mediated triple radical sorting.

formed nickel complex (Tp*)Ni(acac). Meanwhile, the resulting Ir(II) reduces 2-chloro-2,2-difluoroacetamide (**30**) via SET to afford an electrophilic radical (**31**), which can selectively add into an unactivated alkene (**32**), leading to the formation of a sterically hindered 3° alkyl radical **33**. Finally, a favorable $S_H2$ reaction between **33** and the (Tp*)Ni(III)−methyl intermediate delivers the desired dialkylated product with high efficiency and selectivity. This reaction not only tolerates a variety of electrophilic radicals, including the trifluoromethyl radical generated from $dMesSCF_3(OTf)$ [dimesityl(trifluoromethyl)sulfonium trifluoromethanesulfonate] by single electron reduction,[62] but also enables the coupling of various 1° alcohols as the nucleophilic radical precursors. A wide range of mono-, di-, and trisubstituted alkenes bearing reactive functional groups, such as 3° amines, alcohols, and aryl halides, including complex alkene-containing natural products, can be successfully difunctionalized to rapidly access C($sp^3$)-rich small molecule libraries.

In 2024, the Koh group concurrently developed a nickel/photoredox dual catalytic strategy for the trimolecular cross-coupling of alkenes with electron-deficient alkyl halides and phenyliodonium dicarboxylates (Figure 20).[63] Upon photoexcitation of 4CzIPN, triplet energy transfer (TTEnT) activates the iodonium diacetate to release two equiv of methyl radical, one of which is captured by the (Tp*)Ni(II) complex. The other equivalent of methyl radical can engage in XAT with the alkyl iodide **34** to form an electrophilic radical **35**, which undergoes Markovnikov-selective addition to an unactivated alkene to yield a more hindered alkyl radical **36**. The subsequent $S_H2$ reaction of **36** with the (Tp*)Ni(III)−alkyl intermediate forms the desired product. This methodology was applied successfully across a variety of alkenes for the addition of fluoroalkyl, α-acylalkyl, and α-cyanoalkyl radicals as the electrophilic component. The remarkable functional group tolerance is highlighted via the late-stage functionalization of drug- and natural product-derived substrates.

Having demonstrated "triple radical sorting" in the context of alkene dialkylation, we next expanded this general strategy to achieve the aryl-alkylation of alkenes using aryl bromides and 1° alkyl RAEs (Figure 21).[64] In this transformation, the excited Ir(III) photocatalyst (**Ir-2**) oxidizes aminosilane reagent **4** via SET to ultimately generate electron-rich silyl radical **5** and Ir(II). Facile XAT between **5** and aryl bromide **37** releases the electrophilic aryl radical, which undergoes favorable addition to unactivated alkene **32** to reveal nucleophilic 3° alkyl radical **38**. Concurrently, the Ir(II) complex reduces the RAE to furnish the 1° alkyl radical upon the N−O bond cleavage and decarboxylation. Steric radical sorting by the nickel catalyst results in the selective capture of the 1° radical and subsequent $S_H2$ between the 3° radical and the Ni(III)−alkyl intermediate, providing the desired QCC product in good yields. A broad scope of electron-deficient and heterocyclic aryl bromides, small-chain alkyl RAEs, and alkenes of distinct substitution patterns could be coupled successfully,


https://doi.org/10.1021/jacs.5c07367
J. Am. Chem. Soc. 2025, 147, 23351−23366

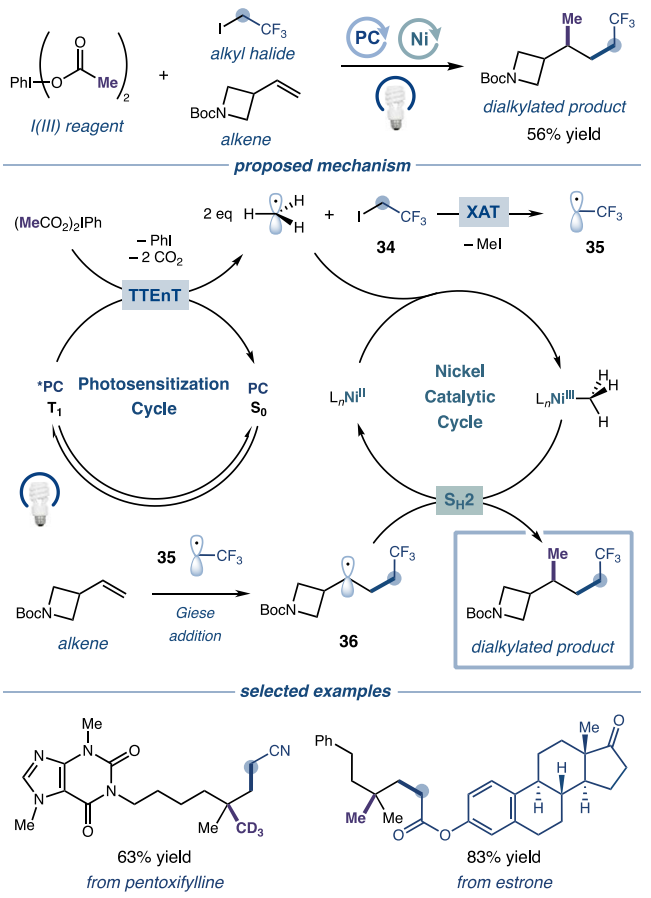


**Figure 20.** Metallaphotoredox-catalyzed regioselective dialkylation of alkenes with alkyl halides and I(III) reagents via an $S_H2$-mediated triple radical sorting.

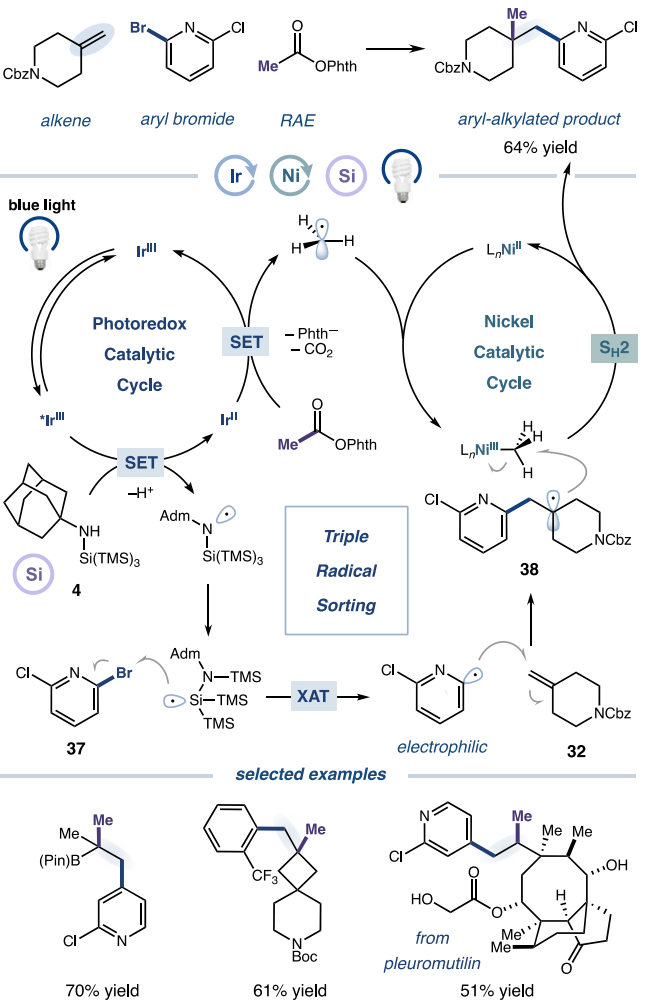


**Figure 21.** Metallaphotoredox-catalyzed regioselective aryl-alkylation of alkenes via an $S_H2$-mediated triple radical sorting.

enabling the rapid enrichment of a pharmaceutically relevant $C(sp^3)$-rich chemical space.

Overall, these "triple radical sorting" protocols demonstrate the power of $S_H2$ radical sorting principles to facilitate the efficient and modular synthesis of highly complex $C(sp^3)$-rich molecular architectures. These systems exhibit excellent tunability and a broad substrate scope and are expected to find immediate applications in synthetic methodology development.[65,66]

## 6. CONCLUSIONS AND OUTLOOK

The introduction of new $C(sp^3)$–$C(sp^3)$ cross-coupling methods remains a major priority for synthetic organic chemists, particularly due to the impetus to expand access to a pharmaceutically relevant $C(sp^3)$-rich chemical space. Bimolecular homolytic substitution ($S_H2$) has recently emerged as a powerful mechanistic paradigm for $C(sp^3)$–$C(sp^3)$ cross-coupling due to its ability to circumvent the limitations of traditional inner sphere reductive elimination. Indeed, $S_H2$ strategies have been proven to offer unprecedented access to $C(sp^3)$-enriched motifs, especially QCCs, from abundant aliphatic precursors. This approach is unified by the intermediacy of distinct open-shell radical intermediates whose reactivity can be effectively differentiated via the application of radical sorting principles to achieve highly cross-selective couplings. Notably, radical sorting strategies have enabled challenging single functional group cross-couplings and three-component alkene difunctionalizations.

Our experiences in this field have taught us that multiple factors contribute to the feasibility and selectivity of $S_H2$ bond-forming processes, including the electronic and steric properties of the radicals, the unique ligand structures of the $S_H2$ catalysts, and the strength of the metal–carbon bond. More specifically, iron porphyrins, nickel tris(pyrazolyl)borates, nickel diketonates, and cobalt salen complexes have emerged as the most effective catalyst scaffolds to support the $S_H2$ $C(sp^3)$–$C(sp^3)$ bond-forming mechanism. These metal–alkyl bonds are often reasonably weak (~10 to 30 kcal/mol) but strong enough to persist without homolysis prior to a successful $S_H2$ reaction. A closer examination of the examples expounded in this perspective reveal that $S_H2$ has proved effective to forge 3°–1° and 3°–Me $C(sp^3)$–$C(sp^3)$ bonds for QCC construction. These trends raise questions about the potential of $S_H2$ catalysts to forge other traditionally challenging connections, such as 3°–2° and 3°–3° $C(sp^3)$–$C(sp^3)$ bonds.[67] Additionally, previous studies suggest that $S_H2$ may also be a plausible mechanism for a number of other transformations, including $C(sp^3)$–X bond formation, especially in the context of enzymatic $C(sp^3)$–H hydroxylation[68] and halogenation reactions[69] and metal-catalyzed epoxidations,[70] aziridinations,[71] and cyclopropanations.[72] Despite the extensive efforts invested in the development of $S_H2$-mediated $C(sp^3)$–X bond formation,[73] the construction of challenging


https://doi.org/10.1021/jacs.5c07367
J. Am. Chem. Soc. 2025, 147, 23351–23366

$C(sp^3)-NR_2$ and $C(sp^3)-OR$ bonds remains largely underexplored.[74,75]

Realization of the above novel reactivities entails significant efforts devoted to the discovery and optimization of ligand architectures that tune the reactivity of the metal catalyst. Furthermore, while $S_H2$ has been shown to be a viable mechanistic step for some first-row transition metals (mainly iron, nickel, and cobalt), other metals may also support this reactivity, including second- and third-row metals, which tend to form stronger metal−carbon bonds and may thus be able to form complexes with more sterically congested carbon centers. Of note, metals from the IIIB and IVB groups, such as ytterbium, scandium, and zirconium, were reported recently to exhibit $S_H2$ $C(sp^3)-C(sp^3)$ bond-forming reactivities when redox-active ligand scaffolds were employed[76,77] (not covered in this perspective). Copper, a prominent first-row transition metal for carbon−heteroatom bond formation in traditional cross-couplings,[78,79] when combined with unique chiral tridentate anionic ligands, has also been shown to promote $S_H2$-mediated enantioconvergent $C(sp^3)-S$ bond formation using challenging 2° and 3° alkyl halide substrates.[80] These recent advancements provide further insights into the impact of ligand design on promoting the desired $S_H2$ reactivities, particularly in the context of sterically hindered coupling partners.[81]

While $S_H2$ radical sorting offers a powerful platform for cross-coupling, several challenges remain. Nickel-based systems preferentially engage less stabilized carbon-centered radicals, leading to a reduced cross-coupling efficiency with benzylic and other stabilized radicals. Both nickel- and iron-catalyzed reaction systems also exhibit diminished productivity with highly $\alpha$-substituted carbons, largely due to steric hindrance. Moreover, current $S_H2$ radical sorting technologies have rarely enabled the formation of 3°−2° or 3°−3° $C(sp^3)-C(sp^3)$ bonds. Ongoing efforts in our laboratory and others aim to overcome these limitations.

We hope this perspective has provided our views on the significant impact of emerging $S_H2$ radical sorting platforms. We are optimistic about these possibilities and look forward to the continued efforts of our group and others to explore the underlying mechanisms and further advance synthetic methodologies enabled by $S_H2$ and radical sorting catalysis. We expect that $S_H2$ will continue to find broader applications in the development of new $C(sp^3)-C(sp^3)$ cross-coupling strategies and beyond.

## AUTHOR INFORMATION


### Corresponding Author

**David W. C. MacMillan** − *Merck Center for Catalysis, Princeton University, Princeton, New Jersey 08544, United States;* orcid.org/0000-0001-6447-0587; Email: dmacmill@princeton.edu

### Authors

**Iona M. McWhinnie** − *Merck Center for Catalysis, Princeton University, Princeton, New Jersey 08544, United States;* orcid.org/0009-0008-4452-0370

**Robert T. Martin** − *Merck Center for Catalysis, Princeton University, Princeton, New Jersey 08544, United States*

**Jiaxin Xie** − *Merck Center for Catalysis, Princeton University, Princeton, New Jersey 08544, United States;* orcid.org/0000-0002-5066-3553

**Ruizhe Chen** − *Merck Center for Catalysis, Princeton University, Princeton, New Jersey 08544, United States*

**Cesar N. Prieto Kullmer** − *Merck Center for Catalysis, Princeton University, Princeton, New Jersey 08544, United States*

Complete contact information is available at: https://pubs.acs.org/10.1021/jacs.5c07367

### Author Contributions

†I.M.M., R.T.M. and J.X. contributed equally. The manuscript was written through contributions of all authors. All authors have given approval to the final version of the manuscript.


### Notes

The authors declare the following competing financial interest(s): D.W.C.M. declares a financial interest with respect to the Integrated Photoreactor.

## ACKNOWLEDGMENTS

Research reported in this work was supported in part by the National Institute for General Medical Sciences of the National Institutes of Health (R35GM134897) and in part by the Office of Naval Research (N000142112138). The authors are grateful for the financial support provided by the Princeton Catalysis Initiative and kind gifts from Merck, Janssen, Bristol-Myers Squibb, Genentech, Genmab, and Pfizer. The content is solely the responsibility of the authors and does not necessarily represent the official views of the NIGMS. I.M.M. and R.C. acknowledge Princeton University, E. Taylor, and the Taylor family for an Edward C. Taylor fellowship. R.T.M. thanks the National Science Foundation for financial support through the MPS-Ascend Postdoctoral Research Fellowship (grant no. 2316541). R.C. thanks the William G. Bowden Merit Fellowship for a graduate fellowship. The authors thank Dr. Nathan W. Dow, Dr. Nicholas E. Intermaggio, and Johnny Wang for helpful discussions and Rebecca Lambert for assistance with the preparation and editing of this manuscript.

## REFERENCES


(1) *Metal-Catalyzed Cross-Coupling Reactions and More*; De Meijere, A., Bräse, S., Oestreich, M., Eds.; Wiley VCH, 2014.

(2) Uehling, M. R.; King, R. P.; Krska, S. W.; Cernak, T.; Buchwald, S. L. Pharmaceutical Diversification via Palladium Oxidative Addition Complexes. *Science* **2019**, *363* (6425), 405−408.

(3) Johansson Seechurn, C. C. C.; Kitching, M. O.; Colacot, T. J.; Snieckus, V. Palladium-Catalyzed Cross-Coupling: A Historical Contextual Perspective to the 2010 Nobel Prize. *Angew. Chem., Int. Ed.* **2012**, *51* (21), 5062−5085.

(4) Choi, J.; Fu, G. C. Transition Metal−Catalyzed Alkyl-Alkyl Bond Formation: Another Dimension in Cross-Coupling Chemistry. *Science* **2017**, *356* (6334), No. eaaf7230.

(5) Kranthikumar, R. Recent Advances in $C(sp^3)-C(sp^3)$ Cross-Coupling Chemistry: A Dominant Performance of Nickel Catalysts. *Organometallics* **2022**, *41* (6), 667−679.

(6) Lovering, F.; Bikker, J.; Humblet, C. Escape from Flatland: Increasing Saturation as an Approach to Improving Clinical Success. *J. Med. Chem.* **2009**, *52* (21), 6752−6756.

(7) Lovering, F. Escape from Flatland 2: Complexity and Promiscuity. *Med. Chem. Commun.* **2013**, *4* (3), 515−519.

(8) Jana, R.; Pathak, T. P.; Sigman, M. S. Advances in Transition Metal (Pd,Ni,Fe)-Catalyzed Cross-Coupling Reactions Using Alkyl-Organometallics as Reaction Partners. *Chem. Rev.* **2011**, *111* (3), 1417−1492.

(9) Chernyshev, V. M.; Ananikov, V. P. Nickel and Palladium Catalysis: Stronger Demand than Ever. *ACS Catal.* **2022**, *12* (2), 1180−1200.
(10) Campeau, L.-C.; Hazari, N. Cross-Coupling and Related Reactions: Connecting Past Success to the Development of New Reactions for the Future. *Organometallics* **2019**, *38* (1), 3−35.
(11) Cheng, L.-J.; Mankad, N. P. C−C and C−X Coupling Reactions of Unactivated Alkyl Electrophiles Using Copper Catalysis. *Chem. Soc. Rev.* **2020**, *49* (22), 8036−8064.
(12) Zhang, Q.; Liu, X.-Y.; Zhang, Y.-D.; Huang, M.-Y.; Zhang, X.-Y.; Zhu, S.-F. Iron-Catalyzed $C(sp^3)$−$C(sp^3)$ Coupling to Construct Quaternary Carbon Centers. *J. Am. Chem. Soc.* **2024**, *146* (8), 5051−5055.
(13) Li, J. Cobalt-Catalyzed C−C Coupling Reactions with $Csp^3$ Electrophiles. In *C-C Cross Couplings with 3d Base Metal Catalysts*; Wu, X.-F., Ed.; Springer International Publishing: Cham, 2023; pp 113−144.
(14) Chan, A. Y.; Perry, I. B.; Bissonnette, N. B.; Buksh, B. F.; Edwards, G. A.; Frye, L. I.; Garry, O. L.; Lavagnino, M. N.; Li, B. X.; Liang, Y.; Mao, E.; Millet, A.; Oakley, J. V.; Reed, N. L.; Sakai, H. A.; Seath, C. P.; MacMillan, D. W. C. Metallaphotoredox: The Merger of Photoredox and Transition Metal Catalysis. *Chem. Rev.* **2022**, *122* (2), 1485−1542.
(15) Yan, M.; Kawamata, Y.; Baran, P. S. Synthetic Organic Electrochemical Methods Since 2000: On the Verge of a Renaissance. *Chem. Rev.* **2017**, *117* (21), 13230−13319.
(16) Tsou, T. T.; Loots, M.; Halpern, J. Kinetic Determination of Transition Metal-Alkyl Bond Dissociation Energies: Application to Organocobalt Compounds Related to B12 Coenzymes. *J. Am. Chem. Soc.* **1982**, *104* (2), 623−624.
(17) Lin, Q.; Spielvogel, E. H.; Diao, T. Carbon-Centered Radical Capture at Nickel(II) Complexes: Spectroscopic Evidence, Rates, and Selectivity. *Chem* **2023**, *9*, 1295−1308.
(18) Hartwig, J. F. *Organotransition Metal Chemistry: From Bonding to Catalysis*; University Science Books: Sausalito, CA, 2010; p 1127.
(19) Xue, W.; Jia, X.; Wang, X.; Tao, X.; Yin, Z.; Gong, H. Nickel-Catalyzed Formation of Quaternary Carbon Centers Using Tertiary Alkyl Electrophiles. *Chem. Soc. Rev.* **2021**, *50* (6), 4162−4184.
(20) Wang, Y.; Begley, T. P. Mechanistic Studies on CysS−A Vitamin B12-Dependent Radical SAM Methyltransferase Involved in the Biosynthesis of the Tert-Butyl Group of Cystobactamid. *J. Am. Chem. Soc.* **2020**, *142* (22), 9944−9954.
(21) Mosimann, H.; Kräutler, B. Methylcorrinoids Methylate Radicals—Their Second Biological Mode of Action? *Angew. Chem., Int. Ed.* **2000**, *39* (2), 393−395.
(22) (a) Che, C.-M.; Lo, V. K.-Y.; Zhou, C.-Y.; Huang, J.-S. Selective Functionalisation of Saturated C−H Bonds with Metalloporphyrin Catalysts. *Chem. Soc. Rev.* **2011**, *40* (4), 1950−1975. (b) Gupta, B. D.; Roy, S. Homolytic Displacement at Carbon. Part 3. First Example of $\alpha$-Attack on the Allenyl- and Prop-2-ynyl-cobaloximes. *J. Chem. Soc., Perkin Trans.* **1988**, *2*, 1377−1383.
(23) Vaillancourt, F. H.; Yeh, E.; Vosburg, D. A.; Garneau-Tsodikova, S.; Walsh, C. T. Nature's Inventory of Halogenation Catalysts: Oxidative Strategies Predominate. *Chem. Rev.* **2006**, *106* (8), 3364−3378.
(24) (a) Johnson, M. D. Bimolecular Homolytic Displacement of Transition-Metal Complexes from Carbon. *Acc. Chem. Res.* **1983**, *16* (9), 343−349. (b) Ashcroft, M. R.; Bury, A.; Cooksey, C. J.; Davies, A. G.; Gupta, B. D.; Johnson, M. D.; Morris, H. Homolytic Displacement at Carbon: V. Formation of Cyclopropylcarbinylsulphones and Trichloroethylcyclopropanes from But-3-enyl Cobaloximes by a Novel Process Involving Homolytic Attack at the $\delta$-Carbon of the Butenyl Ligand. *J. Organomet. Chem.* **1980**, *195* (1), 89−104.
(25) Liu, W.; Lavagnino, M. N.; Gould, C. A.; Alcázar, J.; MacMillan, D. W. C. A Biomimetic $S_H2$ Cross-Coupling Mechanism for Quaternary $sp^3$-Carbon Formation. *Science* **2021**, *374* (6572), 1258−1263.
(26) Daikh, B. E.; Finke, R. G. The Persistent Radical Effect: A Prototype Example of Extreme, 105 to 1, Product Selectivity in a Free-Radical Reaction Involving Persistent $^{\bullet}$CoII[Macrocycle] and Alkyl Free Radicals. *J. Am. Chem. Soc.* **1992**, *114* (8), 2938−2943.
(27) Parsaee, F.; Senarathna, M. C.; Kannangara, P. B.; Alexander, S. N.; Arche, P. D. E.; Welin, E. R. Radical Philicity and Its Role in Selective Organic Transformations. *Nat. Rev. Chem.* **2021**, *5* (7), 486−499.
(28) Zhang, Y.; Li, K.; Huang, H. Bimolecular Homolytic Substitution ($S_H2$) at a Transition Metal. *ChemCatChem* **2024**, *16* (21), No. e202400955.
(29) Zhu, S. F.; Zhang, Q. Transition-Metal-Catalyzed $C(sp^3)$−$C(sp^3)$ Cross-Coupling to Construct All-Carbon Quaternary Carbon Centers. *Synthesis* **2024**, *57*, 1415−1428.
(30) Smith, R. T.; Zhang, X.; Rincón, J. A.; Agejas, J.; Mateos, C.; Barberis, M.; García-Cerrada, S.; De Frutos, O.; MacMillan, D. W. C. Metallaphotoredox-Catalyzed Cross-Electrophile $Csp^3$−$Csp^3$ Coupling of Aliphatic Bromides. *J. Am. Chem. Soc.* **2018**, *140* (50), 17433−17438.
(31) Le, C.; Liang, Y.; Evans, R. W.; Li, X.; MacMillan, D. W. C. Selective $sp^3$ C−H Alkylation via Polarity-Match-Based Cross-Coupling. *Nature* **2017**, *547* (7661), 79−83.
(32) Collman, J. P.; Boulatov, R.; Sunderland, C. J.; Fu, L. Functional Analogues of Cytochrome c Oxidase, Myoglobin, and Hemoglobin. *Chem. Rev.* **2004**, *104* (2), 561−588.
(33) Riordan, C. G.; Halpern, J. Kinetics, Mechanism and Thermodynamics of Iron Carbon Bond Dissociation in Organoiron Porphyrin Complexes. *Inorg. Chim. Acta* **1996**, *243* (1), 19−24.
(34) Gould, C. A.; Pace, A. L.; MacMillan, D. W. C. Rapid and Modular Access to Quaternary Carbons from Tertiary Alcohols via Bimolecular Homolytic Substitution. *J. Am. Chem. Soc.* **2023**, *145* (30), 16330−16336.
(35) Dong, Z.; MacMillan, D. W. C. Metallaphotoredox-Enabled Deoxygenative Arylation of Alcohols. *Nature* **2021**, *598* (7881), 451−456.
(36) Pace, A. L.; Xu, F.; Liu, W.; Lavagnino, M. N.; MacMillan, D. W. C. Iron-Catalyzed Cross-Electrophile Coupling for the Formation of All-Carbon Quaternary Centers. *J. Am. Chem. Soc.* **2024**, *146* (48), 32925−32932.
(37) Li, L.-J.; Zhang, J.-C.; Li, W.-P.; Zhang, D.; Duanmu, K.; Yu, H.; Ping, Q.; Yang, Z.-P. Enantioselective Construction of Quaternary Stereocenters via Cooperative Photoredox/Fe/Chiral Primary Amine Triple Catalysis. *J. Am. Chem. Soc.* **2024**, *146* (13), 9404−9412.
(38) Zhang, B.; Gao, Y.; Hioki, Y.; Oderinde, M. S.; Qiao, J. X.; Rodriguez, K. X.; Zhang, H.-J.; Kawamata, Y.; Baran, P. S. Ni-Electrocatalytic $Csp^3$−$Csp^3$ Doubly Decarboxylative Coupling. *Nature* **2022**, *606* (7913), 313−318.
(39) Gan, X.; Zhang, B.; Dao, N.; Bi, C.; Pokle, M.; Kan, L.; Collins, M. R.; Tyrol, C. C.; Bolduc, P. N.; Nicastri, M.; Kawamata, Y.; Baran, P. S.; Shenvi, R. Carbon Quaternization of Redox Active Esters and Olefins by Decarboxylative Coupling. *Science* **2024**, *384* (6691), 113−118.
(40) Dao, N.; Shenvi, R. A. On the Role of Thermally Activated EDA Complexes in Decarboxylative Cross-Coupling. *Tetrahedron* **2024**, *166*, 134204.
(41) Yan, M.; Lo, J. C.; Edwards, J. T.; Baran, P. S. Radicals: Reactive Intermediates with Translational Potential. *J. Am. Chem. Soc.* **2016**, *138* (39), 12692−12714.
(42) Bour, J. R.; Ferguson, D. M.; McClain, E. J.; Kampf, J. W.; Sanford, M. S. Connecting Organometallic Ni(III) and Ni(IV): Reactions of Carbon-Centered Radicals with High-Valent Organonickel Complexes. *J. Am. Chem. Soc.* **2019**, *141* (22), 8914−8920.
(43) Tsymbal, A. V.; Bizzini, L. D.; MacMillan, D. W. C. Nickel Catalysis via $S_H2$ Homolytic Substitution: The Double Decarboxylative Cross-Coupling of Aliphatic Acids. *J. Am. Chem. Soc.* **2022**, *144* (46), 21278−21286.
(44) Barreiro, E. J.; Kümmerle, A. E.; Fraga, C. A. M. The Methylation Effect in Medicinal Chemistry. *Chem. Rev.* **2011**, *111*, 5215−5246.


https://doi.org/10.1021/jacs.5c07367
J. Am. Chem. Soc. 2025, 147, 23351−23366

(45) Vasilopoulos, A.; Krska, S. W.; Stahl, S. S. C($sp^3$)-H Methylation Enabled by Peroxide Photosensitization and Ni-Mediated Radical Coupling. *Science* **2021**, *372*, 398−403.
(46) Tan, J.-F.; Kang, Y. C.; Hartwig, J. F. Catalytic undirected methylation of unactivated C($sp^3$)−H bonds suitable for complex molecules. *Nat. Commun.* **2024**, *15*, 8307.
(47) Mao, E.; MacMillan, D. W. C. Late-Stage C($sp^3$)−H Methylation of Drug Molecules. *J. Am. Chem. Soc.* **2023**, *145* (5), 2787−2793.
(48) Yuan, M.; Song, Z.; Badir, S. O.; Molander, G. A.; Gutierrez, O. On the Nature of C($sp^3$)−C($sp^2$) Bond Formation in Nickel-Catalyzed Tertiary Radical Cross-Couplings: A Case Study of Ni/Photoredox Catalytic Cross-Coupling of Alkyl Radicals and Aryl Halides. *J. Am. Chem. Soc.* **2020**, *142* (15), 7225−7234.
(49) Sakai, H. A.; MacMillan, D. W. C. Nontraditional Fragment Couplings of Alcohols and Carboxylic Acids: C($sp^3$)−C($sp^3$) Cross-Coupling via Radical Sorting. *J. Am. Chem. Soc.* **2022**, *144* (14), 6185−6192.
(50) Chen, R.; Intermaggio, N. E.; Xie, J.; Rossi-Ashton, J. A.; Gould, C. A.; Martin, R. T.; Alcázar, J.; MacMillan, D. W. C. Alcohol-Alcohol Cross-Coupling Enabled by $S_H2$ Radical Sorting. *Science* **2024**, *383* (6689), 1350−1357.
(51) Green, S. A.; Matos, J. L. M.; Yagi, A.; Shenvi, R. A. Branch-Selective Hydroarylation: Iodoarene−Olefin Cross-Coupling. *J. Am. Chem. Soc.* **2016**, *138* (39), 12779−12782.
(52) Crossley, S. W. M.; Obradors, C.; Martinez, R. M.; Shenvi, R. A. Mn-, Fe-, and Co-Catalyzed Radical Hydrofunctionalizations of Olefins. *Chem. Rev.* **2016**, *116* (15), 8912−9000.
(53) Giese, B. Formation of CC Bonds by Addition of Free Radicals to Alkenes. *Angew. Chem., Int. Ed.* **1983**, *22* (10), 753−764.
(54) Kotesova, S.; Shenvi, R. A. Inner- and Outer-Sphere Cross-Coupling of High $Fsp^3$ Fragments. *Acc. Chem. Res.* **2023**, *56* (21), 3089−3098.
(55) Dao, N.; Gan, X.; Shenvi, R. A. Metal-Hydride C−C Cross-Coupling of Alkenes Through a Double Outer-Sphere Mechanism. *J. Org. Chem.* **2024**, *89* (22), 16106−16113.
(56) Green, S. A.; Huffman, T. R.; McCourt, R. O.; Van Der Puyl, V.; Shenvi, R. A. Hydroalkylation of Olefins to Form Quaternary Carbons. *J. Am. Chem. Soc.* **2019**, *141* (19), 7709−7714.
(57) Gan, X.; Kotesova, S.; Castanedo, A.; Green, S. A.; Møller, S. L. B.; Shenvi, R. A. Iron-Catalyzed Hydrobenzylation: Stereoselective Synthesis of (−)-Eugenial C. *J. Am. Chem. Soc.* **2023**, *145* (29), 15714−15720.
(58) Kong, L.; Gan, X.; Van Der Puyl Lovett, V. A.; Shenvi, R. A. Alkene Hydrobenzylation by a Single Catalyst That Mediates Iterative Outer-Sphere Steps. *J. Am. Chem. Soc.* **2024**, *146* (4), 2351−2357.
(59) Cai, Q.; McWhinnie, I. M.; Dow, N. W.; Chan, A. Y.; MacMillan, D. W. C. Engaging Alkenes in Metallaphotoredox: A Triple Catalytic, Radical Sorting Approach to Olefin-Alcohol Cross-Coupling. *J. Am. Chem. Soc.* **2024**, *146* (18), 12300−12309.
(60) Yamaguchi, Y.; Hirata, Y.; Higashida, K.; Yoshino, T.; Matsunaga, S. Cobalt/Photoredox Dual-Catalyzed Cross-Radical Coupling of Alkenes via Hydrogen Atom Transfer and Homolytic Substitution. *Org. Lett.* **2024**, *26* (23), 4893−4897.
(61) Wang, J. Z.; Lyon, W. L.; MacMillan, D. W. C. Alkene Dialkylation by Triple Radical Sorting. *Nature* **2024**, *628* (8006), 104−109.
(62) Zhang, C. Recent Advances in Trifluoromethylation of Organic Compounds Using Umemoto's Reagents. *Org. Biomol. Chem.* **2014**, *12* (34), 6580−6589.
(63) Cong, F.; Sun, G.-Q.; Ye, S.-H.; Hu, R.; Rao, W.; Koh, M. J. A Bimolecular Homolytic Substitution-Enabled Platform for Multicomponent Cross-Coupling of Unactivated Alkenes. *J. Am. Chem. Soc.* **2024**, *146* (15), 10274−10280.
(64) Wang, J. Z.; Mao, E.; Nguyen, J. A.; Lyon, W. L.; MacMillan, D. W. C. Triple Radical Sorting: Aryl-Alkylation of Alkenes. *J. Am. Chem. Soc.* **2024**, *146* (23), 15693−15700.
(65) Lyon, W. L.; Wang, J. Z.; Alcázar, J.; MacMillan, D. W. C. Aminoalkylation of Alkenes Enabled by Triple Radical Sorting. *J. Am. Chem. Soc.* **2025**, *147* (3), 2296−2302.
(66) Xing, Z.; Liu, F.; Feng, J.; Yu, L.; Wu, Z.; Zhao, B.; Chen, B.; Ping, H.; Xu, Y.; Liu, A.; Zhao, Y.; Wang, C.; Wang, B.; Huang, X. Synergistic Photobiocatalysis for Enantioselective Triple-Radical Sorting. *Nature* **2025**, *637* (8048), 1118−1123.
(67) Yang, W.; Zhao, Z.; Lan, Y.; Dong, Z.; Chang, R.; Bai, Y.; Liu, S.; Li, S.; Niu, L. Heterocoupling Two Similar Benzyl Radicals by Dual Photoredox/Cobalt Catalysis. *Angew. Chem., Int. Ed.* **2025**, *64*, No. e202421256.
(68) Huang, X.; Groves, J. T. Beyond Ferryl-Mediated Hydroxylation: 40 Years of the Rebound Mechanism and C−H Activation. *J. Biol. Inorg. Chem.* **2017**, *22* (2), 185−207.
(69) Petrone, D. A.; Ye, J.; Lautens, M. Modern Transition-Metal-Catalyzed Carbon−Halogen Bond Formation. *Chem. Rev.* **2016**, *116* (14), 8003−8104.
(70) Linker, T. The Jacobsen−Katsuki Epoxidation and Its Controversial Mechanism. *Angew. Chem., Int. Ed.* **1997**, *36* (19), 2060−2062.
(71) Olivos Suarez, A. I.; Jiang, H.; Zhang, X. P.; de Bruin, B. The Radical Mechanism of Cobalt(II) Porphyrin-Catalyzed Olefin Aziridination and the Importance of Cooperative H-Bonding. *Dalton Trans.* **2011**, *40* (21), 5697−5705.
(72) Wang, X.; Zhang, P. X. Catalytic Radical Approach for Selective Carbene Transfers via Cobalt(II)-Based Metalloradical Catalysis. In *Transition Metal-Catalyzed Carbene Transformations*; Wang, J., Che, C., Doyle, M. P., Eds.; Wiley, 2022; pp 25−66.
(73) Nemoto, D. T., Jr.; Bian, K.-J.; Kao, S.-C.; West, J. G. Radical Ligand Transfer: A General Strategy for Radical Functionalization. *Beilstein J. Org. Chem.* **2023**, *19* (1), 1225−1233.
(74) Wang, S.; Li, T.; Gu, C.; Han, J.; Zhao, C.-G.; Zhu, C.; Tan, H.; Xie, J. Decarboxylative Tandem C-N Coupling with Nitroarenes via $S_H2$ Mechanism. *Nat. Commun.* **2022**, *13* (1), 2432.
(75) Lee, W. C.; Zhang, X. P. Metalloradical Catalysis: General Approach for Controlling Reactivity and Selectivity of Homolytic Radical Reactions. *Angew. Chem., Int. Ed.* **2024**, *63* (20), No. e202320243.
(76) Belli, R. G.; Tafuri, V. C.; Joannou, M. V.; Roberts, C. C. D0Metal-Catalyzed Alkyl−Alkyl Cross-Coupling Enabled by a Redox-Active Ligand. *ACS Catal.* **2022**, *12* (5), 3094−3099.
(77) Belli, R. G.; Tafuri, V. C.; Roberts, C. C. Improving Alkyl−Alkyl Cross-Coupling Catalysis with Early Transition Metals through Mechanistic Understanding and Metal Tuning. *ACS Catal.* **2022**, *12* (15), 9430−9436.
(78) Zhu, X.; Chiba, S. Copper-Catalyzed Oxidative Carbon−Heteroatom Bond Formation: A Recent Update. *Chem. Soc. Rev.* **2016**, *45* (16), 4504−4523.
(79) Bhunia, S.; Pawar, G. G.; Kumar, S. V.; Jiang, Y.; Ma, D. Selected Copper-Based Reactions for C−N, C−O, C−S, and C−C Bond Formation. *Angew. Chem., Int. Ed.* **2017**, *56* (51), 16136−16179.
(80) Tian, Y.; Li, X.-T.; Liu, J.-R.; Cheng, J.; Gao, A.; Yang, N.-Y.; Li, Z.; Guo, K.-X.; Zhang, W.; Wen, H.-T.; Li, Z.-L.; Gu, Q.-S.; Hong, X.; Liu, X.-Y. A General Copper-Catalysed Enantioconvergent C($sp^3$)−S Cross-Coupling via Biomimetic Radical Homolytic Substitution. *Nat. Chem.* **2024**, *16* (3), 466−475.
(81) Sterling, A. J.; Ciccia, N. R.; Guo, Y.; Hartwig, J. F.; Head-Gordon, M. Mechanistic Insights into the Origins of Selectivity in a Cu-Catalyzed C−H Amidation Reaction. *J. Am. Chem. Soc.* **2024**, *146* (9), 6168−6177.


https://doi.org/10.1021/jacs.5c07367
J. Am. Chem. Soc. 2025, 147, 23351−23366